8-2013

TOPOLOGY OPTIMIZATION USING A LEVEL SET PENALIZATION WITH CONSTRAINED TOPOLOGY FEATURES

Luis Fernandez
Clemson University, luisf@clemson.edu

TOPOLOGY OPTIMIZATION USING A LEVEL SET PENALIZATION WITH CONSTRAINED TOPOLOGY FEATURES

A Thesis
Presented to
the Graduate School of
Clemson University

In Partial Fulfillment
of the Requirements for the Degree
Master of Science
Mechanical Engineering

---

by
Luis Felipe Fernandez Ayala
August 2013

Accepted by:
Dr. Georges M. Fadel, Committee Chair
Dr. Lonny Thompson
Dr. Rui Qiao
Dr. Paolo Guarneri

ABSTRACT

Topology optimization techniques have been applied to structural design problems in order to determine the best material distribution in a given domain. The topology optimization problem is ill-posed because optimal designs tend to have infinite number of holes. In order to regularize this problem, a geometrical constraint, for instance the perimeter of the design (i.e., the measure of the boundary of the solid region, length in 2D problems or the surface area in 3D problems) is usually imposed. In this thesis, a novel methodology to solve the topology optimization problem with a constraint on the number of holes is proposed. Case studies are performed and numerical tests evaluated as a way to establish the efficacy and reliability of the proposed method.

In the proposed topology optimization process, the material/void distribution evolves towards the optimum in an iterative process in which discretization is performed by finite elements and the material densities in each element are considered as the design variables. In this process, the material/void distribution is updated by a two-step procedure. In the first step, a temporary density function, $\phi^*(\mathbf{x})$, is updated through the steepest descent direction. In the subsequent step, the temporary density function $\phi^*(\mathbf{x})$ is used to model the next material/void distribution, $\chi^*(\mathbf{x})$, by means of the level set concept. With this procedure, holes are easily created and quantified, material is conveniently added/removed.

If the design space is reduced to the elements in the boundary, the topology optimization process turns into a *shape* optimization procedure in which the boundaries are allowed to move towards the optimal configuration. Thus, the methodology proposed

in this work controls the number of holes in the optimal design by combining both topology and shape optimization.

In order to evaluate the effectiveness of the proposed method, 2-D minimum compliance problems with volume constraints are solved and numerical tests performed. In addition, the method is capable of handling very general objective functions, and the sensitivities with respect to the design variables can be conveniently computed.

DEDICATION

This thesis is dedicated to my parents. Without their unconditional love and support, none of this would have been accomplished.

ACKNOWLEDGMENTS

It is a pleasure to thank the many people who made this thesis possible. In the first place, I would like to express my sincere gratitude to my advisor Dr. Georges Fadel for all his support and guidance during this journey. I will always be thankful for his wisdom and overall coaching.

I would like to express the deepest appreciation to Dr. Paolo Guarneri to his persistent help during my master's program and thesis. Thanks for the excellent guidance, review and feedback.

I am deeply thankful to my committee members Dr. Lonny Thompson and Dr. Rui Qiao for their time and contributions. Also, I want to express my gratitude to Dr. Jean-Marc Delhaye for his mentoring and feedback during these two years.

This work would not have been possible without the help and advice of the CEDAR group. All have helped in one way or another to make this work possible, contributing substantially to my ideas and research direction. Special recognition is due to Mr. Ivan Mata for his feedback, constructive advice and countless hours reading this manuscript.

I would like to thank my family for their ever-present love, care, and encouragement.

Finally, I want to thank the Fulbright Foundation and the Ecuadorian National Secretariat of Science, Technology and Innovation, SENECYT, by the scholarship which made possible this master's studies.

TABLE OF CONTENTS

Page

Table of Contents (Continued)

Page

Table of Contents (Continued)

Page

LIST OF TABLES

Table Page

LIST OF FIGURES

Figure Page

List of Figures (Continued)

Page

List of Figures (Continued)

Page

List of Figures (Continued)

Page

List of Figures (Continued)

Page

List of Figures (Continued)

Page

List of Figures (Continued)

Page

NOMENCLATURE

$\mathbf{x}$	Point in the design space
D	Design space
$\phi(\mathbf{x})$	Level set function
$\chi(\mathbf{x})$	Characteristic function
χ_e	Characteristic function in the element e
$\chi_{\min}$	Weak phase fraction to model void domain
C	Threshold constant for the level set penalization
L_C	Level set using the threshold C
L^+_C	Super level set using the threshold C
Ω	Material domain
Γ	Boundary of the material distribution in a given domain
Γ_L	Material-void boundary
Γ_D	Material-design domain boundary
δW	Virtual work done by external forces
δU_e	Virtual deformation energy
$\mathbf{t}$	Vector of traction forces
$\mathbf{b}$	Vector of body forces
$\mathbf{u}$	Vector of displacements
$\mathbf{v}$	Vector of virtual displacements
ϵ_{ij}	Strain tensor

Nomenclature (Continued)

σ_{ij}	Stress tensor
$E_{ijkl}(\mathbf{x})$	Elasticity tensor
$\rho(\mathbf{x})$	Density function
E^{0}_{ijkl}	Elasticity tensor for a solid isotropic base material
$a(\mathbf{u},\mathbf{v})$	Bilinear form
$l(\mathbf{v})$	Linear form
$\mathbf{k_0}$	Stiffness matrix for an element with unit Young Modulus
$\mathbf{k}_{\mathbf{e}\ mat}$	Stiffness matrix for an element filled with material
E	Young modulus for isotropic materials
N	Poisson's Ratio
U	Global displacement vector
V	Global virtual displacement vector
K	Global stiffness matrix
F	Global force vector
U	Space of any admissible displacement
p	Power used in the SIMP method
∇	Spatial gradient
v	Speed in the level set method
t	Time in the level set method

Nomenclature (Continued)

$V(\chi)$	Volume of the material domain
V_0	Volume of the design domain
f	Prescribed volume fraction
N	Number of elements
λ	Lagrange multiplier for the volume constraint
dV	Volume added/removed in the optimization process
α	Linear search parameter
F_{obj}	General objective function
L	Lagrangian
S	Sensitivities
n_h	number of holes
χ_b	Characteristic function of the material-void boundary elements

CHAPTER ONE: INTRODUCTION

1.1 Motivation

Since 1988, with the pioneer work by Bendsoe and Kikuchi [1], the topology optimization method for continuum structures has been an active research area and has been applied to many industrial problems. Topology optimization (TO) is a powerful design tool which finds the optimal material distribution (i.e., optimal structural configuration) in a given domain. Topology optimization of solid structures involves the determination of features such as the number and location and shape of holes and the connectivity of the domain [2]. Different approaches to solve the topology optimization problem have been studied and implemented along these years.

The TO problem can be ill-posed, and lacks a solution in general because optimal designs tend to have an infinite number of holes. For example, if the structural goal is to maximize the stiffness of a structure with a given volume constraint, the introduction of more holes without changing the volume improves its stiffness. Also, this issue leads to numerical instabilities like checkerboards patterns that are undesired. Discretizing the domain in N finite elements, considering each element material or void, is a common practice in the literature of TO, and, the larger the number of elements N, the larger the number of holes that can appear for the optimal solutions. The TO problem is ill-posed basically because it lacks a finite set of feasible designs. In order to regularize this problem, either a geometrical constraint (e.g., perimeter) or a topological constraint (e.g., number of holes) must be imposed. Constraining the number of holes bounds the set of feasible designs. However, in the literature there are no methods that constrain the

number of holes explicitly.

Overcoming the numerical instabilities and defining a well-posed problem (i.e., a problem for which one or more solutions exist) are the motivations to impose a constraint on the number of holes in the designs of the TO problem. The gap in the literature, about methods to constraint the number of holes explicitly, gives a great research opportunity. Current methods in the literature do not control the number of holes obtained in the optimal designs directly. The perimeter constraint method requires perimeter bound values [3]. Ultimately, the optimal solution with a perimeter constraint has a certain finite number of holes, that number is not known until the solution is obtained. On the other hand, other methods incorporate an energy term in the objective to control the "complexity" of the optimal designs and require a regularization parameter [4] [5] [6]. This energy term is related to the shape of the design. This parameter allows exploring different solutions for different number of holes, but there is no direct relationship between the regularization parameter and the specific number of holes obtained. This thesis proposes a procedure to obtain optimal configurations with a desired number of holes.

It should be noted that designs with a large number of holes are difficult or almost impossible to manufacture. The designer should be able to specify the number or the maximum number of holes allowed for the solution, determining the "complexity" level of the design. More holes means more complexity to manufacture and usually results in structures with thinner beam-like elements at low weight. Most of the systems work better if they are kept simple rather than complex, and unnecessary complexity is usually

avoided in design according to the simplicity rule in design [7]. Hence designers should always aim at the minimum number of components with the simplest shapes [7]. These ideas encourage us to obtain optimal topologies with a limited number of holes, and to compare their performance with topologies with more holes. The number of holes is a feature of the material distribution which incorporates a topology constraint. However, the location, shape, size of the holes as well as the connectivity of the domain must be obtained. Besides obtaining optimal topologies with a specific number of holes, this thesis explores the effectiveness of the number of holes in the performance of the structures.

1.2 Hypotheses and Research Questions

In the current literature, different methods to do topology optimization have been studied as well as methods to regularize the ill-posed nature of the topology optimization problem. This thesis investigates a method that solves the topology optimization problem with a constraint on the number of holes explicitly with the following research questions:

1.2.1 Research questions

The main focus of the work is directed to answer one question: Is it possible to formulate a topology optimization problem with a constraint on the number of holes?

To answer this question, several sub-questions can be derived. They are:

a. If it is possible to reformulate the topology optimization problem can a method be constructed to obtain the solution?

   Again, to derive the method, the question can be decomposed in two:

i. How can the number of holes be controlled in the optimization process?

ii. Can a gradient descent method be used in the algorithm to update the designs and decrease faster the objective?

If this first sub-question (a) is answered, a natural extension is:

b. Does the problem have a numerically stable solution?

and if the solution is stable,

c. Is it possible to prove local optimality? i.e. are the positions, shapes, and sizes of these holes in the solution locally optimal?

The research questions are addressed by the following hypotheses to be confirmed in this thesis:

1.2.2 Primary Hypotheses

In the topology optimization problem, constraining the number of holes bounds the set of feasible designs. The topology optimization problem with a constraint on the number of holes is well-posed and solutions are numerically stable.

In the topology optimization problem, if a constraint on the number of holes in a design is imposed, a method can be devised to obtain optimal designs.

1.2.3 Secondary Hypotheses

In order to control the number of holes, the topology optimization method should obtain material/void distribution at every step of the optimization process rather than intermediate densities. The number of holes can be counted easily if each element is either material or void (1/0) in a discrete domain. Gradient methods, used to solve

optimization problems, update the material distribution with intermediate densities. Thus, configurations with intermediate densities obtained by the gradient methods can be penalized towards material/void (1/0) configurations using the level set concept. Thus, holes can easily counted and controlled if the material distribution is described using level sets.

The number, position, shape and size of the holes in the optimal configurations affect the performance of the designs. Since, the number of holes is imposed, the topology optimization method deals basically with the position, shape and size of the holes.

1.3 Dissertation Outline

The remainder of this thesis is organized as follows:

Chapter Two provides an overview of the literature, including topology optimization methods and problem formulation.

Chapter Three details the topology optimization methodology used. Providing the optimization setup, the procedure to obtain the sensitivities, the explanation of the level set penalization, and proposes the topology optimization algorithm.

Chapter Four describes the implementation of the topology optimization algorithm. Also, the question of the methodology to constraint the number of holes in the topology optimization problem is addressed and the respective algorithm and results are provided.

Chapter Five provides concluding remarks and the suggested directions of future work.

CHAPTER TWO: LITERATURE REVIEW

2.1 Topology Optimization

Optimization is a powerful, design-improvement tool that systematically helps the designer to find the design that maximizes or minimizes some criterion or criteria while satisfying some constraint(s). Computer-aided optimization processes aim to reduce design time, improve quality, and deal with large number of repetitive operations. Two main components can be distinguished in the optimization process: the analysis and the design update. The analysis determines the response of a specified system, and the design update defines new designs, hopefully better than the previous ones. Analysis tools such as Finite Elements Analysis (FEA), Computational Fluid Dynamics (CFD) and others validate designs by testing if they fail or if they produce an expected performance. In the optimization process, alternative designs are analyzed in order to find the optimal solution that meets the needs [8].

Specifically, structural optimization can be classified into: sizing, shape, topometry, topography, and topology optimization (see Figure 2.1).

- Sizing finds the best dimensions for elements like bars, beams, or mechanical parts. Sizing usually deals with a few number of design variables.
- Shape optimization tools obtain the best possible shape of a structure, modifying its external contour.
- Topometry optimization finds the optimal distribution of the elements' dimensions in a given designable domain [9], it can be seen as an "element by

element" sizing optimization problem. Topometry usually deals with a large number of design variables.

- Topography optimization is an advance form of shape optimization in which the shape is improved with the location of internal patterns, for example, the bend patterns in a sheet metal part [10].
- Lastly, topology optimization obtains the best possible distribution of material in a design domain [2].

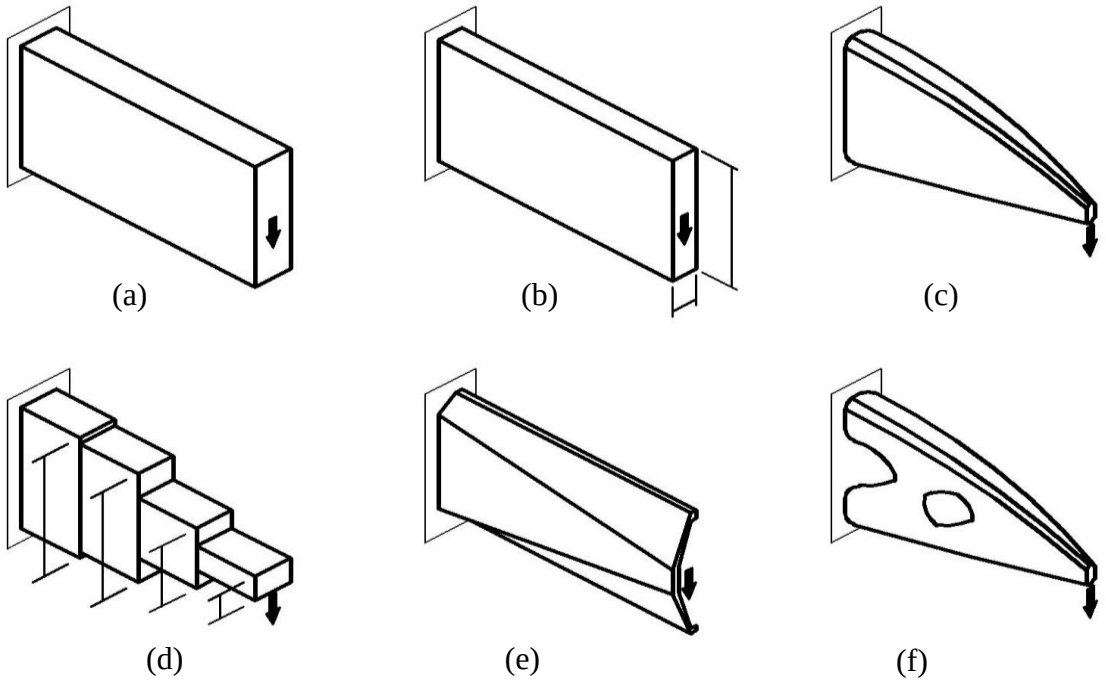

Figure 2.1: Structural optimization schematic classification, a) Design domain and problem b) Sizing optimization c) Shape optimization d) Topometry optimization e) Topography optimization f) Topology optimization.

The topology of a structure, i.e., the arrangement of the material, is crucial for its structural performance. At the early stages of the design process, it is desired and

necessary to improve the quality of a product and reduce costs by finding the best possible topology of that product.

TO started with the pioneer work of Michell [11] back in 1904. Michell developed a design theory for the optimal layout of thin-bar trusses that minimized their weight. As seen in Figure 2.2, the bars in the optimal structures are all perpendicular to each other and the maximum tensile or compressive stress governs the arrangement of the structure. Important extensions and implementations were made by Prager [12] [13], Rozvany and Prager [14] using the optimality criteria, i.e. conditions for the optimal design.

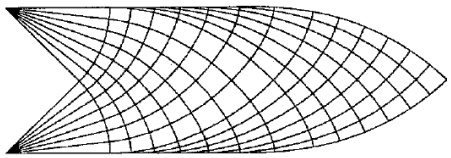

Figure 2.2: Michell-cantilever. Representation of the analytical solution of the least-weight truss for a cantilever with point load [15].

TO can be divided into discrete and continuous. A discrete structure (i.e., truss) is a set of (designable) elements or members (i.e., bars). For discrete structures, the optimum topology determines the best number, position and connectivity of the structural members. On the other hand, a continuum structure is a continuous mass that completely fills the space it occupies (i.e., solid objects). For continuum structures the optimum topology determines the external shape as well as the internal boundaries and inner holes with respect to a design objective and constraints [16]. Because the focus of this work is the topology optimization of continuum structures, this literature review covers exclusively continuum structures. For more comprehensive reviews on TO of continuum

structures, the reader is referred to the works of Eschenauer and Olhoff [16], Hassani and Hinton [17], Bendsoe and Sigmund [2] and Rozvany [18].

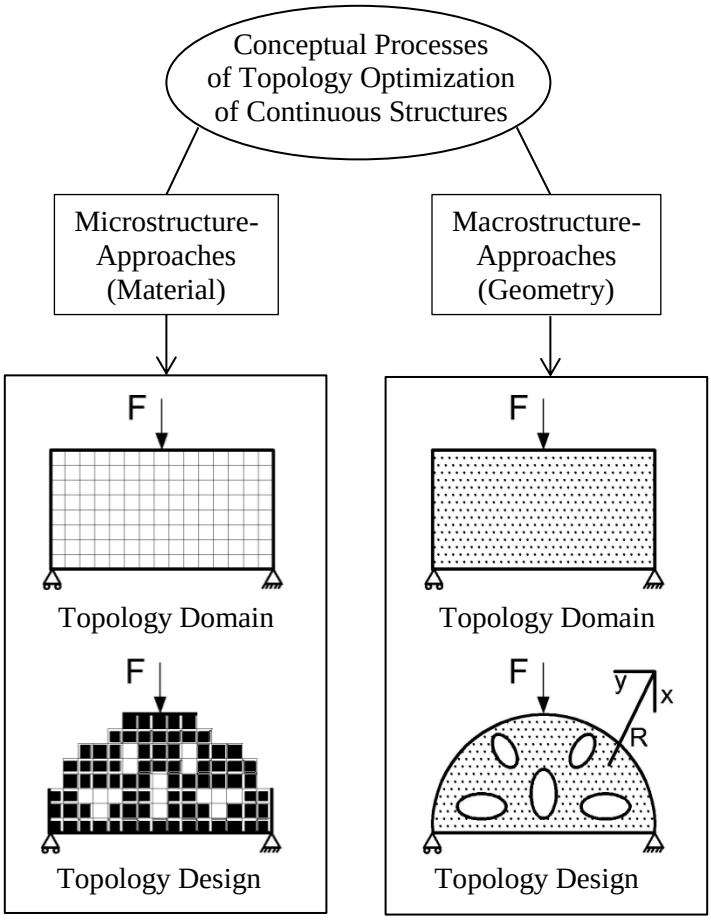

Figure 2.3: Conceptual processes of topology optimization [16].

TO of continuum structures can be classified into Micro and Macro approaches (see Figure 2.3) [16]. Microstructure approaches use a fixed finite element mesh to describe the geometry and the mechanical behavior. The finite elements have constitutive properties using a relationship between the material stiffness tensor and the material density based on the physical modeling of the porous microstructures. In other words, the properties of the micro-structured or porous material are related to the microstructure

dimensions and shape, therefore its density. Since the material properties are related with the microstructure and the optimization process consists in determining the elements that should have material or not, this method is also called Material approach. Thus, the density of material in each element is used as a design variable defined between the limits 0-void and 1-solid, however the optimization penalizes or pushes towards the limits {0,1}, resulting in a rough description of the boundaries in the continuous domain. Based on this topology, subsequent shape optimization is usually carried out in order to obtain more defined results.

On the other hand, macrostructure approaches do not consider solid materials as porous or micro structured. Since the optimization is carried by defining the geometry of where the material is present, this approach is also called Geometry approach. Thus, the finite element mesh can either be fixed or it can change in the optimization process, allowing changes and creation of new boundaries. In these methods, material from the admissible design domain is appropriately added/removed. Usually holes and boundaries are subjected to shape optimization simultaneously.

2.2 Microstructure approaches

Microstructure approaches are based on material models that allow the density of the material within each element to have intermediate values from 0 (void) to 1 (solid). For example, the material properties of a plate with periodic perforated holes as a microstructure can be modeled as a function of the dimensions of these periodic holes. In order to study the effect of these microstructures in a domain, the homogenization

method is used. Homogenization [19] [20] [21] analyzes a unit cell with given periodicity constraints assuming it is very small compared to the design domain. Using the homogenization method, the relationship between the density of material in the composite (i.e., sizes of holes) and the effective material properties can be obtained. Bendsoe and Kikuchi [1], in their pioneer work, proposed the use of these artificial composite materials with microscopic voids in order to obtain the optimal topology design using a homogenization method. The design space is fixed and divided in a finite element mesh with a periodic repetition of a unit cell. Each cell has its own design variables (i.e., size of the hole) and its material properties relationship can be known using homogenization. Thus, the optimization problem is changed to obtain the parameters that characterize the cells (i.e., sizes of holes) in the design domain (see Figure 2.4). Thus, the optimization problem changes to a sizing problem. The optimal solution has intermediate densities that require a "lumping" or "cut-off" procedure to decide whether these elements should be solid or void in a macroscopic structure. This homogenization design method (HDM) has been applied and studied for different design problems. Also, other techniques like smear-out [22] and quasiconvexification [23] can replace homogenization to obtain the effective mechanical properties of periodic microstructures.

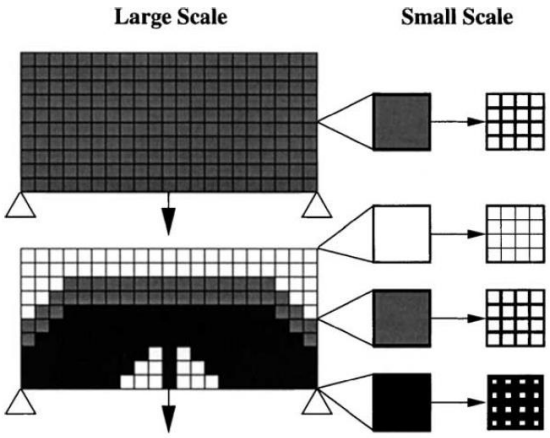

Figure 2.4: Basic concept of HDM using a square microcell with centrally placed rectangular hole as material model. (Top) Before optimization – uniform homogenized material for all Fes and (Bottom) after optimization – each FE has different material density [24].

In the past decade, HDM has been used less frequently, and replaced by the Solid Isotropic Material with Penalization (SIMP) material model [25]. This approach uses an artificial or fictitious material model where the elasticity tensor is given with a power law of the density function given by: $E_{ijkl}(\mathbf{x}) = \rho(\mathbf{x})^p E^0_{ijkl}$, p>1, where $\rho(\mathbf{x})$, $\mathbf{x} \in D$. $0 \le \rho(\mathbf{x}) \le 1$ is a density function of the material, E^0_{ijkl} is the elasticity tensor of a given solid isotropic base material, and D is the design space. In a discrete finite element mesh, the power p>1 lowers the stiffness of the element as an exponential function of its density ρ_e. In this way, this approach effectively penalizes intermediate densities, favoring the creation of more distinctive 0-1 designs. If the power tends to infinity, ρ^p tends to {0,1} (see Figure 2.5). Thus, SIMP is used to approximate the {0,1} problem. Solutions depend on the power p and the mesh. Also, checkerboard patterns appear due to the discretization. However, some of these drawbacks disappear with the use of perimeter or surface constraints, filtering sensitivities techniques, or with a local constraint on the

gradient of the material density. The intermediate densities can be interpreted as elements with microstructures but are difficult or impossible to produce. The SIMP method has been extended successfully to other material interpolations [26] and used for the solution of different design problems.

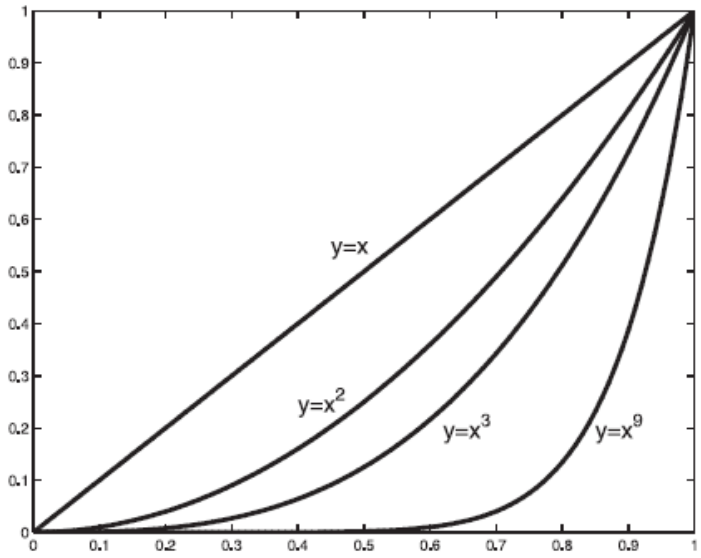

Figure 2.5: The action of the power p. The value of x^p tends to zero for a fixed $x \in [0, 1)$ as p tends to infinity [27].

2.3 Macrostructure approaches

The macrostructure techniques do topological changes by two main approaches: removing/adding material (degenerating and/or growing a structure) and by inserting holes in a structure. [16]

The first main technique, degenerating and/or growing structures, considered that the solution can be obtained by adding/removing material from/to the design domain. In these techniques the design domain is discretized in a ground mesh, and the design variables are the densities of the elements, which are however forced to assume either a 0

or 1 value. First, Rossow and Taylor [28] proposed a variable thickness sheets model. Thus, in a discrete planar sheet, a very close to zero thickness in the elements implies voids. Similarly, Atrek [29] developed the SHAPE method using Lagrange multipliers, the optimality criteria, and the element volumes as design variables. In this technique, the optimization process forces the intermediate volumes to assume 0-1 values internally. Also, an optimality criterion function termed "virtual volume" measures the volume (objective) compared with the most critical factor (constraints). This virtual volume of the current configuration is compared with the one obtained in the previous step. If there is no improvement in the virtual volume (should be smaller), a small increase in the current volume can alleviate the critical factor preventing the optimization process from developing towards a local minimum. Similarly, the Karlsruhe Research Center developed an optimization process simulating the biological growth with the Computer Aided Optimization (CAO) and the Soft Kill Option (SKO) methods. SKO cuts away under stressed sub-domains (remove inefficient material), and the CAO achieves a constant stress distribution. Similar to SKO, Xie and Steven [30] proposed the so-called method of Evolutionary Structural Optimization (ESO) combining an intuitive-heuristic and a gradient-based approach. ESO removes the lowest stressed elements and re-analyzes the structure iteratively until a fully stressed design is obtained. An extension of this method allows adding material where the structure is over stressed calling this method Bidirectional ESO or (BESO).

For all the methods mentioned above, the capability to add/remove material depends on a ground mesh and on its size. In this sense, Liu, Parks and Clarkson [31]

developed a Metamorphic Development (MD) method that does not rely on a ground mesh, and allows adding/removing material through adding/removing nodes/elements during the optimization process. With MD, growth is guided to occur only in certain regions called "growth cones" of the current structure and using network topologies, as shown in Figure 2.6. MD can start from a very basic structure (e.g. plate) and can be used in large scale engineering problems which may be impracticable for ground-mesh based optimization methods [31] .

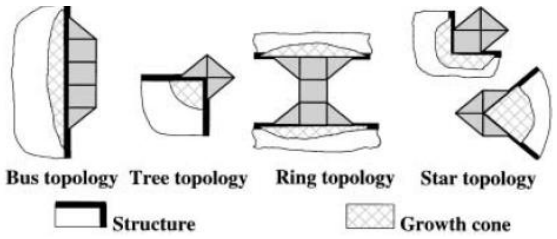

Figure 2.6: Structural growth in growth cones by network topologies [31].

The second main technique is inserting holes in the structure. This technique introduces and positions new small holes or bubbles in the existing structure, and then shape optimization of the boundaries, including the new holes, is carried out with parameterized boundaries. For this technique, the boundaries of the structure are taken as design parameters. In the so-called bubble method, developed by Eschenauer, Kobelev and Schumacher [32], the bubble is positioned at the point of the structure that satisfies a position criterion. This position criterion is derived using calculus of variations, and consists in evaluating a derived "characteristic function" (function of the principal stresses) for each point of the structure; the bubble is positioned at the point of the structure where the characteristic function is the minimum. Following this approach, Garreau et al. [33] derive the topological sensitivities for a large class of cost functions. A

topological sensitivity calculates the variation of the cost function with respect to the creation of the small bubble as a perturbation of the structural domain. These topological sensitivities provide the information of the location to create the bubbles improving the cost function. Sokolowski and Zochowski [34] gave some mathematical justifications to these topological sensitivities.

2.4 Level set methods for topology optimization

The Level set method is considered a non-traditional topology optimization method because the mesh is a fixed grid used to define a scalar function that describes the geometry of the structures "implicitly". As mentioned in the previous sections, the Micro and Macrostructure approaches use a fixed grid with the exception of the metamorphic development (mesh increase/decrease) and the bubble method (mesh can change or mesh free methods can be used). However, in all of these Micro and Macrostructure methods, the geometry is represented "explicitly". Nevertheless, level set methods for topology optimization can be considered as a macroscopic approach (see Figure 2.7).

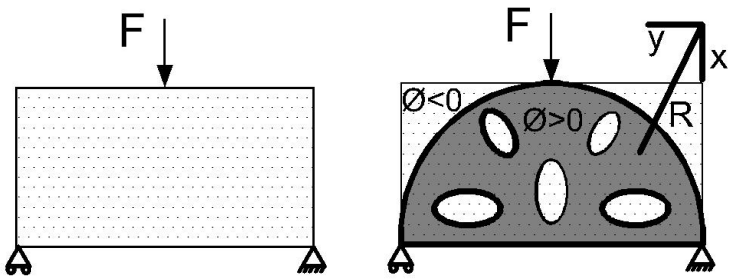

Figure 2.7: (Left) Topology domain. (Right) Topology design using level set function ϕ =0 in the boundary, ϕ >0 material, ϕ <0 void.

The level set method was originally developed by Osher and Sethian in 1988 [35] for numerically tracking the propagation of fronts and free boundaries (see Figure 2.8).

The level set method represents the boundaries implicitly (Γ) as the zero level curve of a grid function so-called "level set function" (ϕ see Equation 1).

$$\Gamma = \{\mathbf{x} \mid \phi(\mathbf{x}) = 0\} \quad \textbf{(1)}$$

To describe the movement of the boundary "Γ" in the normal direction with a speed "v", the level set function "ϕ" satisfies the following level set equation in time "t":

$$\frac{\partial \phi}{\partial t} = v|\nabla \phi| \quad \textbf{(2)}$$

This partial differential equation (PDE) is also known as the Hamilton-Jacobi equation. The evolution or propagation of the boundaries is tracked by solving this PDE numerically in an Eulerian framework (i.e. fixed Cartesian grid) without parameterizing the curves or the object. The normal velocity can be an arbitrary function of the local curvature as in a variety of physical phenomena [35], and in the PDE, viscous terms can be incorporated to model more general time varying objects e.g., viscous fluids. These algorithms are versatile, can be constructed with a desired accuracy, topological merging and breaking occurs naturally (see Figure 2.8), and are useful in a variety of applications such as fluid mechanics, phase transitions, image processing, and solid modeling in CAD.

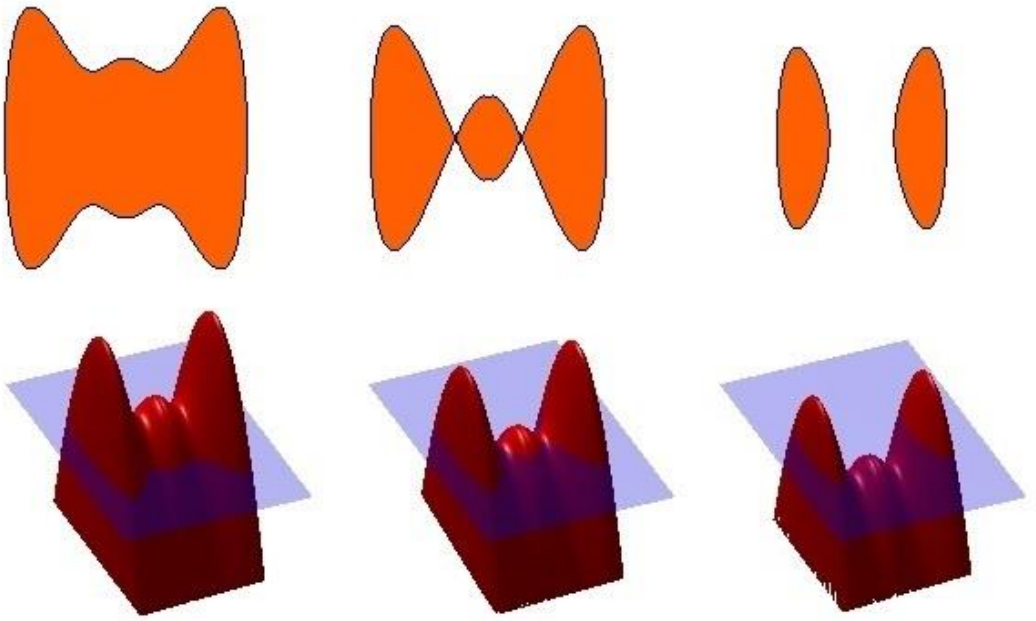

Figure 2.8: Boundary propagation using level set method.

Sethian and Wiegmann [36] first proposed a structural optimization method using the level set approach. First, a level set function is initialized. Then, the equilibrium equations are solved using finite difference techniques for the current configuration. The velocity of the Hamilton-Jacobi equation is used as a function of the Von Mises stresses of the current design, such that the algorithm adds material in regions of high stress and removes it in regions of low stress (Similar to SKO method but using a different evolution technique). Solving this PDE numerically, the level set function is updated. The process is repeated until convergence has been achieved.

Several researchers extended the level set method deriving a velocity function to update the Hamilton-Jacobi equations using the "sensitivities" (i.e., shape derivatives). Osher and Santosa [37] used this optimization strategy with the shape derivatives for solving eigen-frequency problems for a two-density heterogeneous drum. Furthermore,

Wang, Wang, and Guo [38] [39] derived a velocity function using the sensitivities for general objectives and constraints. In their studies, the level set function uses the same mesh as the finite elements used to solve the equilibrium equations. With their proposed method, minimum compliance problems with volume constraints were solved. Using the same approach, Wang and Wang [40] solved multi-material topology optimization problems using a multi-phase modeling referred as "color " level set representation. This approach avoids the problem of overlapping different material phases. Using m independent level set functions, each phase is then defined as a specific combination rule (i.e. [all $\phi_i>0$], or [all $\phi_i<0$], or [$\phi_1<0$, $\phi_2>0$, $\phi_3<0,\ldots$, $\phi_m<0$]) representing up to $n=2^m$ distinct material phases. In their work, 2D minimum compliance problems with two to four material phases were studied. Independently. Allaire, Jouve and Toader [41] [42] also derived shape derivatives and used them in combination with the level-set algorithm to do shape optimization of structures. The displacement field was calculated using an ersatz material model (i.e., fill the holes by a weak phase) and doing finite element analysis.

The level set methods mentioned above were successfully applied to obtain best topologies. However, they have some difficulty to create new holes or they get stuck at shapes with fewer holes than the optimal shapes. To overcome this drawback some researchers incorporated topological derivatives [43] [44] and others did not use the Hamilton-Jacobi evolution equation [45] [4].

In this sense, Allaire et al. [43] extended the level set method using a "topology gradient", based on the bubble method (discussed in section 2.3), in order to allow the

creation of new holes. These techniques have been applied to two and three dimensional, linear and non-linear elastic problems, targeting minimum compliance, vibrations and/or multiple loads [46]. Also, Burger et al. [44] in an independent work derived and incorporated topological derivatives into the level set method.

Belystchko, Xiao and Parimi [45] used the Heaviside function of a level set function (implicit function) to describe the shape (density) of a design. The level set function is defined in terms of nodal variables and C^0 (i.e., continuous across boundaries) finite element shape functions. To solve the equilibrium equation, an extended finite element approach "X-FEM" [47] is used. The Heaviside function is regularized in order to obtain the sensitivities of the objectives and constraints numerically, and these gradients are used to update the implicit function. Structural examples were implemented for single and multi-material problems. The level set function with C^0 shape functions ensures continuity across the elements, but not on the derivative, suggesting that the mesh must be sufficiently fine, or it will lead to high numerical errors defining the sensitivities.

Similarly, Wang and Wang [48] used a "superimposed" finite element method (instead of FEA or finite difference method) to improve the results to track the boundaries in the level set method.

Amstutz and Andra [49] noted that the nature of the Hamilton-Jacobi evolution equation allows merging and cancellation of the holes but the nucleation of new holes seems to be rather unlikely. The Hamilton-Jacobi equation, as it was mentioned earlier, models well the movement of the "boundaries" with a given normal velocity. And if the level set function is bounded (e.g., between -1 and +1) the gradient term tends to zero

$|\nabla\phi| \to 0$ in the object, so there is no change in time of the level set in the object (see equation 2). Thus, these authors use an evolutionary equation based on the topological gradient instead of the Hamilton-Jacobi equation obtaining satisfactory results to nucleate new holes in the optimization process.

Some issues can still be noticed in these methods: the mesh dependency, the solution of a complicated partial differential equation, numerical accuracy requiring a re-initialization operation of the level set function and the dependency on initial designs. To address some of the issues, many researchers have tried to improve or extend these methods.

For example, Wang et al. [50] [51] incorporated radial basis functions (RBF) with multiquadric (MQ) splines into the conventional level set method to improve its efficiency. Also, with the transformation of the Hamilton-Jacobi equation (PDE), into an ordinary differential equation (ODE) the proposed method was implemented for minimum compliance problems to allow a smooth propagation of the front of the implicit function avoiding re-initialization and alleviating other issues.

Chen et al. [52] combined parametric shape optimization with topology optimization using the theory of R-functions. The R-functions are also level set functions, and represent implicitly the geometries. In the theory of R-functions, "primitives" (i.e., basic geometries) can be defined with parameters (e.g., radius of a circle) and still represent in an implicit way the geometries. Also, the theory of R-functions allows operations between primitives (and/or level set functions) like union, intersection and subtraction. These authors represent the shapes implicitly with a level set function

defined with B-splines, and combined with parameterized geometries using the R-functions to support desired parametric changes. For the solution of the equilibrium equations, a mesh free method developed by the authors is used. Solutions examples of topology optimization combined with shape parametric optimization were successfully obtained.

Luo et al. [5] and Chen et al. [6] employed a quadratic energy functional in the objective of the topology optimization which introduces geometric information and realizes shape feature control of the width of the structural components obtained. The optimal structure obtained is a network of interconnected beam elements where the width of the beams is likely the same and can be controlled. The methods have been implemented for minimum compliance structures and compliant mechanisms in two dimensions. This method imposes implicitly a constraint on the width of the structural components regularizing the TO problem.

Wei and Wang [53] used a piecewise constant level set function, keeping the advantages of the implicit representation of the geometry and defining the density as a piecewise function. Also, instead of updating with the Hamilton-Jacobi equation, a simple gradient method is used. Optimal designs were obtained for minimum compliance problems without the need to solve a PDE, and without the re-initialization of the level set function.

Another different technique to model the material distribution is the phase field. The phase field model is used to represent the surface dynamics of phase transition phenomena, i.e., solid-liquid transitions. This model was initially proposed by Cahn and

Hilliard [54], and Allen and Cahn [55] in order to represent the interfacial energy of a mixture of fluids. The phase field model has been extended and used in many dynamic simulations of multi-phase flow, crack propagation, interface tracking, etc. Bourdin and Chambolle were the first to apply the phase field method to structural optimization [56] [57]. In this method, a phase field function is allowed to take any real value in the design domain, and ideally should take just the different boundary phase values (e.g., 0-void 1-solid). Thus, the energy of the interface between the phases is measured using the so called Cahn and Hilliard equation. This energy is included in the topology optimization process in order to force the phase field function to take boundary phase values. This method initially was used to implement perimeter constraints, however the advantages of obtaining topologies with no intermediate densities attracted many researchers and have been studied and extended [58] [59] [60]. The phase field model itself does not incorporate topological changes (new holes), basically it is a surface tracking method.

Rong and Liang [61] used a dynamic level set model to update the level set function instead of the Hamilton-Jacobi equation. A nonlinear velocity mapping using the concept of the conjugate gradient is proposed. Also, a topology mutation and crossover operators based on genetic algorithms approach where implemented to improve the numerical results. In spite of the mixture of these gradient and non-gradient techniques and of the complexity of the algorithm, this method shows fair results without any specific benefit among other implementations.

Yamada et al. [4] proposed a topology optimization method based on the level set method but incorporating a fictitious energy term in the objective function. This fictitious

energy depends on the shape of the level set function ($\nabla^2\phi$) and its use controls implicitly the geometry of the optimal structure. Additionally, instead of the Hamilton-Jacobi equation for the update of the level set function the authors propose that the change of the level set function is proportional to the derivative of the objective function. With this method, minimum compliance problems, compliant mechanisms and vibration problems were solved numerically. The weight parameter of the fictitious energy allows controlling implicitly the geometrical "complexity", that is the number of holes and number of beam-like elements of the optimal solutions.

These level set methods and their extensions have been applied and implemented by many researchers [62] [63] [64] [65] [66] [67]. However, the methods are diverse, and numerical tuning and details are needed to ensure their success in specific cases. There is a lack of what can be considered a general robust level set method approach.

2.5 Well-posed problem formulation

Is it well known that the discrete (0/1) topology optimization problem is ill-posed [16]. Some attempts to solve this problem do not converge to patterns of material and void, or solutions tend towards designs with an infinite number of macroscopic holes. Regularization corrects or approximates solutions of ill-posed problems. Relaxation (i.e., extend the design space) and restriction (i.e., reduce the set of feasible designs) are ways to regularize the ill-posed problems, obtaining well-posed problems or numerically stable solutions.

In the literature, by introducing intermediate densities (as the HDM and SIMP method), the problem is relaxed. In the optimization process intermediate densities are

penalized, and finally some difficulties are alleviated. However, mesh dependency (no convergence), checkerboards, and solutions with large number of holes are still obtained.

According to Sigmund and Petersson [68], common numerical problems appearing in TO are checkerboards, mesh dependency and local minima. Checkerboards denote the problem of formation of regions of alternating solid and void elements in a checkerboard fashion. Mesh dependency refers to the problem of not obtaining qualitatively the same solution for different mesh-sizes or discretization. Local minima refers to the problem of obtaining different solutions to the same discretized problem when choosing different algorithmic parameters.

Heuristic methods as filters of the sensitivities [69] based on image processing techniques have shown to stabilize convergence. The implementation is easy, the computation costless and can be combined with other methods as SIMP. These filters produce dubious optimal designs because the topology optimization problem is still ill-posed. The solution obtained by these filters can be an optimal configuration of a well-posed problem but the specific formulation of the problem is not known.

On the other hand, restriction of the problem can regularize the problem and define a well-posed one. Either a geometrical constraint (e.g., perimeter) or a topological constraint (e.g., number of holes) must be imposed in the TO problem.

If a constraint is imposed on the perimeter of the structure [3], stable results, defined patterns, and configurations with a finite number of holes are obtained. However, predicting the perimeter constraint value can be difficult especially for 3D problems. Since the goal is to obtain optimal topologies, designers usually do not know the

perimeter constraint values for the problem. Also, if the perimeter constraint is too tight, the optimization problem may result in no solution.

Instead of a perimeter constraint, a point wise constraint on the gradient of the density of material can be imposed [70]. This local gradient constraint incorporates 2N (N is the number of elements) extra constraints rendering this method impractical.

Besides these methods, a fictitious energy term in the objective function [4] in a topology optimization method based on the level set method allows also overcoming the ill-posed difficulties. This fictitious energy depends on the shape of the level set function. The weight parameter of the fictitious energy allows controlling the geometrical "complexity", that is, the number of holes and number of beam-like elements of the optimal solutions. However, there is no direct relation between the weight parameter value and the scale of the structure (volume, weight). So, predicting the desired weight is difficult.

Similarly, a quadratic energy functional in the objective of the topology optimization can be incorporated to realize shape feature control of the width of the structural components obtained [5] [6]. This method impose implicitly a constraint on the width of the structural components regularizing the TO problem. The optimal structure obtained is a network of interconnected beam elements where the width of these beams is likely the same and can be controlled.

2.6 Summary

Table 2.1 (extracted from [68]) summarizes the problems found in topology optimization. Table 2.2 summarizes the different techniques of topology optimization of continuum structures.

Table 2.1: Definition of problems found in discretized topology optimization. An "∃" indicates existence of solutions has been proven. [68]

Numerical experience	Mathematical problem	Physical explanation	Prevention techniques
Checkerboards	No convergence of FE-solutions	Erroneous FE-modeling of checkerboards	-Higher order finite elements -Patches -Filtering -Restriction methods below
Mesh dependence **(a) Necessarily finer and finer structure**	(a) Nonexistence	(a) "convergence" to microstructure	(a) -Relaxation (∃) -Perimeter (∃) -Global/local gradient constraint (∃) -Mesh-independent filtering
(b) Possibly finer and finer structure	(b) No uniqueness	(b) Ex.: uniaxial stress	(b) Nothing (maybe manufacturing preferences)
Local minima	No convergence of algorithm	-No convexity -Flatness	Continuation methods

Table 2.2: Summary of topology optimization methods of continuum structures.

	METHOD	MATERIAL	DESIGN VARIABLES	GRADIENT	UPDATE	COMMENTS
MICROSTRUCTURE (MATERIAL) APPROACHES	Homoge-nization	0-gray-1 micro-structures	Sizing of micro-structure parameters	Use	Add/remove mass to element	Porous elements
	SIMP	Penalize gray elements	Densities of elements	Use	Add/remove mass to element	Versatile, and robust defined, depend on p
	Other material interpolation model	Penalize gray elements	Densities of elements	Use	Add/remove mass to element	Depend on inter-polation
MACROSTRUCTURE (GEOMETRY) APPROACHES	Degenerate add/or grow structure	0/1	Elements or parametric curves	Some use	Add/remove element	Heuristic and gradient
	Insert new holes	0/1	Elements or parametric curves	Use	Move boundaries/ create holes	Not easy to extend to other objectives
	Phase model	0 / 1 (boundary 0-1)	Control points phase function	Some use	Solve evolutionary equation	Track boundaries not new holes
	Level set methods	0 / 1 (boundary 0-1) implicit represen-tation	Control points level set function	Some use	Solve evolutionary equation	Need mechanism to generate holes

In general, according to Rozvany [18], most of the authors in numerical topology optimization simply compare their solutions visually with the exact optimal truss topology and are satisfied with a vague resemblance. This is a very subjective method for verifying topology optimization methods and solution. After this literature review, we

also agree that there is a need for reliable methods with more quantitative confirmation of the benefits and accuracy of the numerical results.

Furthermore, regularization methods such as heuristic filters and the perimeter constraint method have successfully obtained stable numerical results. As it was mentioned in this literature review, these methods have some advantages and disadvantages. However, there is a gap in the current literature, there is no method that imposes a constraint explicitly on the number of holes in the TO problem. A finite and controlled number of holes are obtained by some TO methods implicitly. In these methods, parameters such as the perimeter or weights are related indirectly to the number of holes.

In order to explore this research gap, in this thesis, the TO problem with an imposed constraint on the number of holes is attempted to be solved. The constraint on the number of holes closes the set of feasible designs. Thus, regularizes by restriction the ill-posed problem, defining a well-posed one. A methodology to solve this problem is proposed and quantitative confirmation of the results is presented.

CHAPTER THREE: METHODOLOGY

This chapter explains the use of the level sets to represent the material distribution of a structure. A brief overview of structural static elastic problems is presented. Finally, the methodology to do topology optimization through the use of the level set concept is described in detail.

3.1 Level set function to represent material distribution

The level set of a real scalar function $\phi(\mathbf{x})$ is the set of points $\mathbf{x} \in R^n$, n=1, 2, 3… where the function $\phi(\mathbf{x})$ takes on a constant given value C:

$$L_C\left(\phi(\mathbf{x})\right) = \left\{\mathbf{x} \in \mathbb{R}^n : \phi(\mathbf{x}) = C\right\} \qquad \textbf{(3)}$$

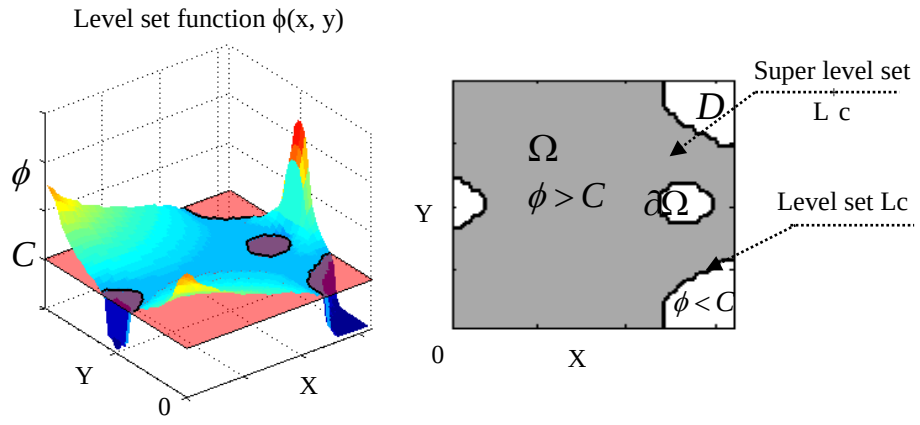

Figure 3.1: Representation of the level set function, the level set Lc and the super level set L^+c.

The scalar function $\phi(\mathbf{x})$ is so-called "level set function" because it takes any point **x** as an input and returns a certain "level" or "height" as an output. Thus, the level set Lc specifies a boundary in an implicit form as the iso-curve(s) (level curve(s), or contour line(s)) of the level set function when n=2 dimensions (see Figure 3.1). However, the

level set specifies a boundary as the iso-surface (or level surface) of the level set function when n=3 dimensions. For higher dimensions the level set is a level hyper-surface.

The "super level set" is defined in the same sense to include all the points **x** on the level set function which are above a level C, including that level C:

$$L^{+}_{C}\left(\phi(\mathbf{x})\right)=\left\{\mathbf{x}\in\mathbb{R}^{n}:\phi(\mathbf{x})\geq C\right\} \qquad \textbf{(4)}$$

This super level set L^{+}_{C} specifies a region in an implicit form as a surface in n=2 dimensions (see Figure 3.1) or a solid in n=3 dimensions.

The main properties of the level sets are [71]:

- The super level set of a convex function is convex (converse is not generally true)
- The gradient of the level set function at a point **x** is perpendicular to the level set of the function at that point.
- A very complicated contour or level set can have a well-behaved (continuous and differentiable) level set function.
- Shape and topological changes (creation of new holes, breaking and merging boundaries) are easily handled by changes of the level set function.
- $\phi(\mathbf{x})-C$ can be interpreted as the distance of the point **x** from the boundary defined by the level set L_C. If $\mathbf{x}\in L_C$, the distance is zero $\phi(\mathbf{x})-C=0$. If $\mathbf{x}\notin L_C$,then $\left|\phi(\mathbf{x})-C\right|>0$.

Topology optimization is a "Boolean" problem that consists in determining the material/void distribution. If x is any point in R^2 or R^3 that belongs to the design domain D, and Γ is the boundary of the material domain Ω, the super level set Lc+ definition

properly fits the topology optimization problem, that is $\mathbf{x}\in$Lc+ represents the region where the material is and $\mathbf{x}\notin$Lc+ represents where void is (see Figure 3.1).

$$\phi(\mathbf{x})\begin{cases} > C & \text{if } \mathbf{x}\in\Omega \\ = C & \text{if } \mathbf{x}\in\partial\Omega \\ < C & \text{if } \mathbf{x}\notin\Omega \end{cases} \qquad \textbf{(5)}$$

3.2 Structural equilibrium equation for linear elastic problems

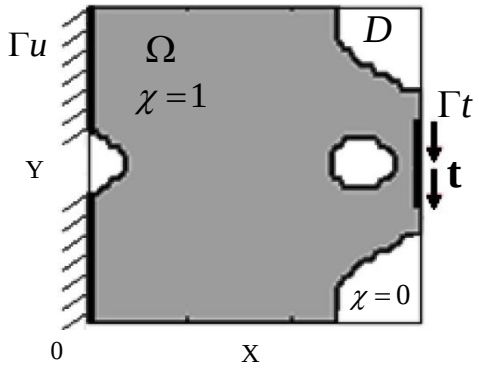

Figure 3.2: Representation of a structural problem and characteristic function of the current configuration.

Linear elastic problems are based on the following assumptions:

- The deformation process is reversible (no permanent deformations occur) and isothermal.
- The load process is quasi-static and the volumes in the deformed/un-deformed bodies are equal.

For the static case, the theorem of virtual displacements states that the virtual work δW of external forces acting on a body equals the increase of the virtual deformation energy δU_e of the body.

$$\delta W_{work} = \delta U_e \qquad \textbf{(6)}$$

Consider a structural mechanical problem, with a material domain Ω in the design domain D. The characteristic function $\chi(\mathbf{x})$ is defined as 1 in the material domain and 0 in void domains (see Figure 3.2):

$$\chi(\mathbf{x}) = \begin{cases} 1 \text{ if } \mathbf{x} \in \Omega \\ 0 \text{ if } \mathbf{x} \in D \setminus \Omega \end{cases} \quad \textbf{(7)}$$

Γ_u is part of boundary of the domain Ω were displacements are given. Traction forces $\mathbf{t}^T = \begin{bmatrix} t_x & t_y & t_z \end{bmatrix}$ are imposed at the boundary Γ_t (see Figure 3.2) and body forces $\mathbf{b}^T = \begin{bmatrix} b_x & b_y & b_z \end{bmatrix}$ are applied through the material domain Ω. The displacement vector of the elastic body at each point is expressed as $\mathbf{u}^T = \begin{bmatrix} u_x & u_y & u_z \end{bmatrix}$ with the respective virtual displacement vector $\mathbf{v}^T = \begin{bmatrix} v_x & v_y & v_z \end{bmatrix}$. The strain tensor is defined as $\boldsymbol{\epsilon}_{ij} = \frac{1}{2}\left(\frac{\partial u_i}{\partial x_j} + \frac{\partial u_j}{\partial x_i} \right)$. The constitutive equation or material law is expressed as $\sigma_{ij} = E_{ijkl}\boldsymbol{\epsilon}_{kl}$

Using the elasticity tensor $\mathbf{E}^0$ of the prescribed material, the virtual energy terms can be defined.

$a(\mathbf{u}, \mathbf{v})$ is defined as the (energy) bilinear form that represents the internal virtual work of an elastic body at the equilibrium displacement **u**, and for an arbitrary virtual displacement **v**. Using the characteristic function χ, the bilinear form can be defined as an integral in the design domain D:

$$a(\mathbf{u}, \mathbf{v}) = \int_{\Omega} \boldsymbol{\epsilon}(\mathbf{u})^T \mathbf{E}^0 \boldsymbol{\epsilon}(\mathbf{v}) \, d\Omega = \int_{D} \boldsymbol{\epsilon}(\mathbf{u}) : \mathbf{E}^0 \chi(\mathbf{x}) : \boldsymbol{\epsilon}(\mathbf{v}) \, d\Omega \quad \textbf{(8)}$$

$l(\mathbf{v})$ is the linear form that represents the external virtual work of the loads for the arbitrary virtual displacement **v**.

$$l(\mathbf{v}) = \int_{\Gamma t} \mathbf{t}^T \mathbf{v}\, d\Gamma + \int_{\Omega} \mathbf{b}^T \mathbf{v}\, d\Omega = \int_{\Gamma_t} \mathbf{t} \cdot \mathbf{v}\, d\Gamma + \int_{D} \chi(\mathbf{x}) \mathbf{b} \cdot \mathbf{v}\, d\Gamma \qquad \textbf{(9)}$$

Using all these definitions, the principle of virtual work or displacement (equation 6) states that:

$$a(\mathbf{u}, \mathbf{v}) = l(\mathbf{v}) \qquad \textbf{(10)}$$

Using the finite element method, the design domain D is discretized in N finite elements. χ_e is the discrete value of the characteristic function in the element e. Thus, χ_e defines if there is material or not in the element e and collectively, χ_1, χ_2,…, χ_N are the design variables of the optimization problem. Defining Ω_e as the domain of the element e:

$$\chi_e = \begin{cases} 1 \text{ if } \Omega_e \in \Omega \\ 0 \text{ if } \Omega_e \in D \setminus \Omega \end{cases} \qquad \textbf{(11)}$$

$\mathbf{u_e}$ and $\mathbf{v_e}$ are the displacement and virtual displacement vectors of the element e. $\mathbf{k_0}$ is the stiffness matrix of an element filled with material. **U** and **V** are the global and virtual displacement vectors respectively. Finally, **K** is the global stiffness matrix, and **F** is the global force vector. The linear and bilinear can be expressed as:

$$a(\mathbf{u}, \mathbf{v}) = \int_{D} \epsilon(\mathbf{u}) : \mathbf{E}^0 \chi(\mathbf{x}) : \epsilon(\mathbf{v})\, d\Omega = \sum_{e=1}^{N} \mathbf{u_e} \mathbf{k_0} \chi_e \mathbf{v_e} = \mathbf{U^T K V} \qquad \textbf{(12)}$$

$$l(\mathbf{v}) = \int_{\Gamma_t} \mathbf{t} \cdot \mathbf{v}\, d\Gamma + \int_{D} \chi(\mathbf{x}) \mathbf{b} \cdot \mathbf{v}\, d\Gamma = \mathbf{F^T V} \qquad \textbf{(13)}$$

Since the virtual displacement $\mathbf{V}$ is arbitrary, using equations 12 and 13 in 10, the discrete equilibrium equation can be reduced to:

$$\mathbf{KU} = \mathbf{F} \qquad \textbf{(14)}$$

Finite element analysis deals with the construction and definition of the element matrices and the assembly to global matrices and vectors (i.e., **K**, **F**, **U**, and **V**) due to the discretized mesh. The solution of the equilibrium equations requires boundary conditions in order to set the given displacement and forces of the structural problem in the equilibrium equation. Then, the displacements of the free nodes of the discretized element mesh are obtained, as well as the reaction forces of the fixed nodes. After solving the equilibrium equations other physical quantities can be obtained such as the stresses, strains, strain energy, compliance, volume, weight, etc. in a post-processing procedure.

The objective and constraints for the topology optimization problem can be defined with these results. A common practice is to minimize the compliance of the structure (work done by external forces) considering certain volume constraint, or to minimize the weight subject to stress constraints for instance, etc. Starting from a current configuration the goal of the approach is to propose a new configuration at each step in which the objective is improved.

3.3 Minimum compliance topology optimization problem with volume constraint

3.3.1 Formulation of the problem

First, let us assume a fixed design domain D with a material domain Ω and a void domain $D\backslash\Omega$. This constitutes the current configuration. Consider the problem of

topology design for minimum compliance (maximum stiffness) of statically loaded linear elastic structures under a single loading condition. The compliance is defined as the work done by the set of given loads against the displacements at equilibrium [16].This external work depends on the loads and obviously on the structure (material distribution), the stiffer the structure the lower the compliance. The compliance can be defined using the linear form $l(\mathbf{u})$. The compliance and the volume (mass) are conflicting. In general, a heavier structure is stiffer. With no constraint on the volume, the optimal solution will be a fully filled design domain D. The objective is to minimize the compliance under a volume constraint:

$$\begin{aligned} \min_{u,\chi} &: l(\mathbf{u}) \\ \text{subject to} &: a(\mathbf{u},\mathbf{v}) = l(\mathbf{v}),\ \forall \mathbf{v} \in U,\ \ \mathbf{u} \in U \\ &: \frac{V(\mathbf{x})}{V_0} \le f \\ &: \chi(\mathbf{x}) = \{0,1\} \end{aligned} \qquad \textbf{(15)}$$

$V(\chi)$, V_0 , and f are the volume, the design domain volume and the prescribed volume fraction respectively. *U* is the space of any admissible displacement. In order to solve problem (15), it is reformulated as the following problem according to the finite element discretization (*I* is the set of elements):

$$\begin{aligned} \min_{\mathbf{U},\chi} &: \mathbf{F}^T\mathbf{U} \\ \text{subject to} &: \mathbf{F} = \mathbf{K}\mathbf{U} \\ &: \frac{V(\chi)}{V_0} \le f \\ &: \chi_i = \{0,1\} \quad i \in I \end{aligned} \qquad \textbf{(16)}$$

Let N define the number of elements. The constrained problem is transformed to an unconstrained problem using Lagrange relaxation, defined as:

$$\min_{\mathbf{U},\mathbf{V},\boldsymbol{\chi}} : L = \mathbf{F}^T\mathbf{U} + \left(\mathbf{F} - \mathbf{K}\mathbf{U}\right)^T \mathbf{V} + \lambda\left(\sum_i^N \frac{\chi_i}{N} - f\right) \qquad \textbf{(17)}$$

$$\text{subject to: } \chi_i = \{0,1\} \quad i \in I$$

Notice that in this case, the vector $\mathbf{V}^T = \begin{bmatrix} V_1 & V_2 & \dots & V_n \end{bmatrix}$ represents a set of Lagrange multipliers that enables us to satisfy each finite element equation as an equality constraint. At the same time, **V** is called the adjoint vector of the mechanical problem, and can be interpreted as pseudo initial displacements because it must have units of displacement. Furthermore, λ is the Lagrange multiplier for the volume constraint.

3.3.2 Sensitivities in the optimization process

The optimality conditions expressed through the Karush-Kuhn-Tucker (KKT) equations are the conditions that must necessarily hold a design to be a local optimum. The KKT equations are:

Stationary conditions

$$\frac{dL}{dU_i} = 0 \qquad \textbf{(18)}$$

$$\frac{dL}{d\chi_i} = 0 \qquad \textbf{(19)}$$

Primal feasibility conditions

$$\mathbf{F} = \mathbf{K}\mathbf{U} \qquad \textbf{(20)}$$

$$\frac{V(\boldsymbol{\chi})}{V_0} - f \le 0 \qquad \textbf{(21)}$$

Dual feasibility

$$\lambda \geq 0 \qquad \textbf{(22)}$$

Complementary slackness

$$\lambda\left(\frac{V(\boldsymbol{\chi})}{V_0} - f\right) = 0 \qquad \textbf{(23)}$$

The primal feasibility conditions hold in every step of the optimization process. The finite element method is used to guarantee the primal feasibility condition by solving the equilibrium equation $\mathbf{F} = \mathbf{KU}$, obtaining the displacement vector **U** for the given configuration.

Also, the first stationary condition $\left(dL/d\mathbf{U} = \mathbf{0}\right)$ is forced to be satisfied at every step of the optimization. Thus, the following equations should hold:

$$\frac{dL}{dU_i} = F_i - K_{ij}V_j = 0 \qquad \mathbf{F} - \mathbf{KV} = 0 \quad \text{Adjoint problem} \qquad \textbf{(24)}$$

The obtained equation 24 is called the adjoint problem because it is similar (or identical) to the equilibrium equation, where **V**, the adjoint displacement, is the unknown. To guarantee the first stationary condition at every step of the optimization process, the adjoint displacements V_j are calculated by solving the adjoint problem of equation 24. Since it is the same problem as the equilibrium equation 20, this is called a self-adjoint problem, and:

$$\mathbf{V} = \mathbf{U} \qquad \textbf{(25)}$$

On the other hand, the second stationary condition $\left(dL/d\boldsymbol{\chi} = \mathbf{0}\right)$ holds just in local optimal configurations which are the ones that are desired in the optimization process,

and it is not necessary true for the initial (or current) configuration. Satisfying the equilibrium equation and the adjoint problem in the optimization process at every step, the sensitivities of the Lagrangian with respect to the design variables can be calculated as:

$$\frac{dL}{d\chi_i} = \frac{\partial}{\partial \chi_i}\left[\mathbf{F}^T\mathbf{U} + \mathbf{F}^T\mathbf{V} - \mathbf{U}^T\mathbf{K}\mathbf{V} + \lambda\left(\sum_e^N \frac{\chi_e}{N} - f\right)\right] + \\ + \frac{\partial}{\partial u_j}\left[\mathbf{F}^T\mathbf{U} + \mathbf{F}^T\mathbf{V} - \mathbf{U}^T\mathbf{K}\mathbf{V} + \lambda\left(\sum_e^N \frac{\chi_e}{N} - f\right)\right]\frac{\partial u_j}{\partial \chi_i}$$

$$\frac{dL}{d\chi_i} = \frac{\partial}{\partial \chi_i}\left\{-\sum_{e=1}^N \mathbf{u_e}^T\mathbf{k_0}\chi_e\mathbf{v_e} + +\lambda\sum_e^N \frac{\chi_e}{N}\right\} + \frac{\partial}{\partial \mathbf{U}}\left\{\mathbf{F}^T\mathbf{U} - \mathbf{U}^T\mathbf{K}\mathbf{V}\right\}\frac{\partial \mathbf{U}}{\partial \chi_i}$$

$$\frac{dL}{d\chi_i} = -\mathbf{u_i}\mathbf{k_0}\mathbf{v_i} + \frac{\lambda}{N} + \cancel{\left(\mathbf{F} - \mathbf{K}\mathbf{V}\right)}\frac{\partial \mathbf{U}}{\partial \chi_i}$$

It is known according to equation 24 that $\mathbf{F} - \mathbf{K}\mathbf{V} = \mathbf{0}$, then $\mathbf{V} = \mathbf{U}$ at every step. Thus, the steepest direction can be expressed as:

$$\frac{dL}{d\chi_i} = S_i^k = -\mathbf{u_i}^T\mathbf{k_0}\mathbf{u_i} + \frac{\lambda}{N} \qquad \textbf{(26)}$$

3.4 Update techniques for the optimization algorithm

Using the sensitivities of the topology optimization problem, for example Equation 26, the steepest descent direction can be computed to minimize the Lagrangian function L using a linear search. Thus, to update the material distribution, a two-step procedure is proposed:

1) obtain a temporary material density distribution (ϕ), and

2) penalize this new material distribution towards 1/0 material distribution.

The first step, generates the updated material densities (ϕ) with the steepest descent direction, as shown in the equation below:

$$\phi_i = \chi_i^k - \alpha S_i^k \qquad \textbf{(27)}$$

α defines the distance by which to move in the direction S_i^k in the k^{th} iteration. In the optimization process, to improve L, the j^{th} element of the design space D should be removed, maintained or added. However, the updated material densities ϕ_i will not take only the integer values of {0,1}, in general they can be any real number ($\phi_i \in R$), between 1 and 0, higher than 1 and below 0.

In the second step, the updated material densities (ϕ) are used as a level set function. The super level set of the function ($\phi(\mathbf{x}) \geq C$) is used to penalize the intermediate values and obtain a discrete material-void distribution ($\boldsymbol{\chi}^{k+1}$). Thus, elements where $\phi_i \geq C$ jump immediately to $\chi_i^{k+1}=1$, and elements where $\phi_i < C$ drop to $\chi_i^{k+1}=0$. The constant C can be for example 0.5.

$$\chi_i^{k+1} = \begin{cases} 1 \text{ if } \phi_i \geq C \\ 0 \text{ if } \phi_i < C \end{cases} \qquad \textbf{(}28\textbf{)}$$

For different values of α, different configurations are obtained. The selected α should give the best configuration update but the search must be computational efficient. The value of α can be determined mainly in 3 ways:

- Minimize $L(\boldsymbol{\chi}^{k+1}(\alpha))$, which is a tedious problem because the function L is evaluated multiple times for different configurations.

- Add/remove a certain amount of volume $dV(\chi^{k+1}(\alpha))=dV$ at each step. This is simple, but the value of dV is arbitrary and does not guarantee best improvement in L.
- Obtain a configuration with a prescribed number of holes. Usually there is an interval for α which can generate configuration with the same number of holes. Since the configurations are 1/0 designs, counting the number of holes is simple. However, obtaining the desired number of holes in the first iteration is not common. Thus, an algorithm with several iterations is required.

The material distribution $\chi^{k+1}(\alpha^*)$ obtained replaces the old vector of design variables χ^k for the next iteration. In the next chapter, algorithms using these techniques are explained and implemented.

3.5 Shape optimization

Noticing that the material-void boundary Γ_L (see Figure 3.3) is just part of the whole boundary of a defined structure that occupies the material domain $\Omega \subseteq D$,

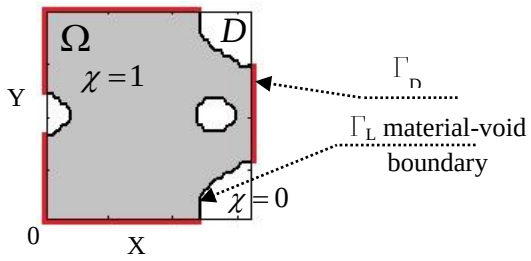

Figure 3.3: Structural boundaries defined by the level set.

the whole boundary of the material domain Ω ($\Gamma_\Omega = \Gamma_L + \Gamma_D$) is defined as the union of the material-void boundary Γ_L and the boundary of the material with the fixed

domain D (Γ_D). To perform shape optimization, only changes in the level set boundary Γ_L are allowed to minimize the compliance. Thus, using the results of the previous sections, the optimization problem is:

$$\begin{aligned} &\min_{\mathbf{U},\chi} : \mathbf{F}^T\mathbf{U} \\ &\text{subject to: } \mathbf{F} = \mathbf{K}\mathbf{U} \\ &\quad : \frac{V(\mathbf{x})}{V_0} \le f \\ &\quad : \chi_i = \{0,1\} \quad \text{for } \chi_j \in \Gamma_L \end{aligned} \tag{29}$$

The Lagrangian and sensitivities are similar to the ones of the topology optimization problem but in (29), the design variables correspond to the boundary elements. A method to define the elements that belong to the boundary Γ_L is needed. In this sense, the gradient with respect to the coordinates (not the design variables) of the characteristic function is different from zero in the boundary Γ_L because the characteristic function changes from 0 to 1 or vice versa at the boundary. So, the design variables that are part of the design space in the optimization process are the ones for which $\nabla\chi(x)\neq 0$. A gradient of χ can be defined, such that it is zero for the elements in the material and void domain excluding the boundary ($\Omega\backslash\Gamma_L$ and $D\backslash\Omega$), using forward and backward finite differences numerically. Note that this gradient is non-zero for all the elements that correspond to Γ_L. In the next chapter, the details of the implementation are explained. The definition of the modulus of the gradient for each discrete design space is:

$$|\nabla\chi_i| = \begin{cases} a & \text{if } \chi_i \in \Gamma_L \\ 0 & \text{if } \chi_i \notin \Gamma_L \end{cases} \tag{30}$$

For the shape optimization problem the design domain is just Γ_L at each iteration step. Thus, all the elements whose modulus of the gradient is different from zero are updated.

$$\phi_i = \chi_i - \alpha \frac{dL}{d\chi_i} \qquad \text{if } |\nabla \chi_i| \neq 0 \qquad \textbf{(31)}$$

This update guarantees changes only in the material-void and not in the material or void domain. With this procedure, no holes are created in the material domain, there is just an evolution of the boundary. However, the boundary changes allow merging and breaking of the boundaries and can produce creation/elimination of new holes (see Figure 3.4).

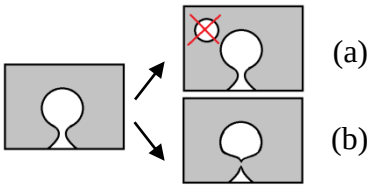

Figure 3.4: Shape optimization: a) no holes are created in the material; b) merging and breaking boundaries can produce new holes.

Since only the design variables updated are the ones with the nonzero gradient, the update equation can be reformulated as:

$$\phi_i = \chi_i - \alpha \frac{dL}{d\chi_i} |\nabla \chi_i| \qquad \textbf{(32)}$$

Eq.(29) is the discrete version of the Hamilton-Jacobi equation used in the level-set method. For a bounded and continuous level set function, the highest values of the modulus of the gradient are in the boundary, and are zero or near zero far from the boundary and inside the domain. Thus, the Hamilton-Jacobi equation easily tracks the

movement of the boundary, but shows difficulties to create holes in the topology optimization because the sensitivities tend to be zero inside the domain producing no-changes inside the domain. This point is highly supported in the literature and many researchers have tried to use different evolutionary equations instead of the Hamilton-Jacobi equation [45] [4] [49]. However, the benefits of separating the topological changes (creation of new holes) from the shape changes can help to control the desired number of holes in the optimal configuration. For example, it may be desired to put some manufacturing restrictions on the maximum number of holes in a structure. A large number of holes using the same amount of material can make a structure stiff but almost impossible to manufacture. As a solution, once the optimization process reaches the desired number of holes, just shape optimization is allowed.

3.6 Sensitivities of a general topology optimization problem

In this section, the sensitivities of a topology optimization to minimize a general objective function are obtained. The optimization process iteratively improves this objective obtaining a better material distribution. The objective function F_{obj} can be any scalar function that depends on the material distribution and the displacements in the deformation state. This is because structural quantities such as the strains, stresses, weight, volume, energy terms, etc., can be defined using the displacements and the material distribution. The displacements are obtained subject to a certain material distribution and the equilibrium equation, so the equilibrium equation is a constraint for any static structural topology optimization problem. χ is the vector of the discrete

characteristic function representing our design variables. The general optimization problem is defined as:

$$\begin{aligned} &\min_{U_j,\chi_i} : F_{obj} = f\left(\boldsymbol{\chi},\mathbf{U}\right) \\ &\text{subject to}: \mathbf{F} = \mathbf{KU} \\ &\qquad\quad : \chi_j = \{0,1\} \end{aligned} \tag{33}$$

The Lagrangian of the problem and the KKT equations are:

$$L = f\left(\boldsymbol{\chi},\mathbf{U}\right) + \left(\mathbf{F}-\mathbf{KU}\right)^T \mathbf{V} \tag{34}$$

Stationary conditions

$$\frac{dL}{dU_i} = 0 \tag{35}$$

$$\frac{dL}{d\chi_i} = 0 \tag{36}$$

Primal feasibility conditions

$$\mathbf{F} = \mathbf{KU} \tag{37}$$

In the optimization process the primal feasibility is achieved by solving the equilibrium equation and obtaining the unknown displacements **U** given the current material distribution. Also, the first stationary condition $\left(dL/d\mathbf{U} = \mathbf{0}\right)$ is forced to be achieved at each step, which turns to be the adjoint problem (obtaining the adjoint displacements **V**):

$$\frac{dL}{dU_i} = 0 = \frac{\partial}{\partial U_i}\left(f\left(\boldsymbol{\chi},\mathbf{U}\right) + \left(\mathbf{F}-\mathbf{KU}\right)^T \mathbf{V}\right)$$

$$\frac{dL}{d\mathbf{U}} = 0 = \frac{\partial}{\partial \mathbf{U}} f\left(\boldsymbol{\chi},\mathbf{U}\right) - \mathbf{KV}$$

If the adjoint force vector is defined as: $\mathbf{F}^{*adj} = \frac{\partial}{\partial \mathbf{U}} f(\chi, \mathbf{U})$, the adjoint problem is similar to the equilibrium equation:

$$\mathbf{F}^{*adj} = \mathbf{KV} \qquad \textbf{(38)}$$

The second stationary condition $(dL/d\chi = 0)$ is only satisfied for local minima. The derivatives of the function L with respect to the variable χ_j can be obtained by:

$$S_j = \frac{dL}{d\chi_j} = \frac{\partial}{\partial \chi_j}\left(f(\chi, \mathbf{U}) + (\mathbf{F} - \mathbf{KU})^T \mathbf{V} \right) + \cancel{\frac{\partial}{\partial U_i}\left(f(\chi, \mathbf{U}) + (\mathbf{F} - \mathbf{KU})^T \mathbf{V} \right) \frac{\partial U_i}{\partial \chi_j}} \qquad \textbf{(39)}$$

If the adjoint displacement **V** is used, obtained by eq. 38, the second term of eq. 39 disappears. Thus, the sensitivities are:

$$S_j = \frac{dL}{d\chi_j} = \frac{\partial}{\partial \chi_j} f(\chi, \mathbf{U}) - \mathbf{u}_j{}^T \mathbf{k_0} \mathbf{v}_j \qquad \textbf{(40)}$$

Using this as the steepest descent direction we can minimize the Lagrangian function L iteratively using the techniques described in section 3.4.

3.7 Summary

In this chapter, a methodology to perform topology optimization was described. The topology optimization problem for minimum compliance with a volume constraint was studied. Using finite elements and considering the material densities in each element as the design variables, a Lagrangian formulation is developed and the sensitivities of the Lagrangian with respect to the design variables are analytically derived in detail for this problem.

In order to minimize the Lagrangian, the material/void distribution is updated by a two-step procedure. In the first step, a temporary density function, $\phi^*(x)$, is updated through the steepest descent direction using sensitivities. In the subsequent step, the temporary density function $\phi^*(x)$ is used to model the next material/void distribution, $\chi^*(x)$, by means of the level set concept. The updated configurations exhibit a 0/1 configuration, consequently holes are easily created and quantified with this procedure.

If the design space is reduced to the elements in the boundary, the topology optimization process turns into a *shape* optimization procedure using the same update technique. Finally, the sensitivities are derived for a topology optimization problem with general objective function to minimize.

In the next Chapter, using these techniques, the algorithms to obtain optimal topologies in an iterative process are explained. Also, the implementations of the algorithms are described and examples are solved.

CHAPTER FOUR: IMPLEMENTATION AND EXAMPLES

In this chapter, the implementation in Matlab of the method proposed in this work is presented. The code includes a Finite Element Analysis, a topology optimization procedure to place a prescribed number of holes and perform shape optimization. Finally, solutions for topology optimization problems for minimum compliance with constrained volume and number of holes are shown.

4.1 Finite Element Analysis (FEA)

The FEA evaluates the current structure given a material distribution. Structural outputs such as displacements, strains, stresses, elastic energy, etc. can be calculated by the FEA. The design domain is assumed rectangular with "xL" width, "yH" height, and it is discretized by "nex" and "ney" elements along the horizontal and vertical directions respectively. The numbering of these rectangular elements starts from the lower left corner, proceeding column by column until the upper right (see Figure 4.1).

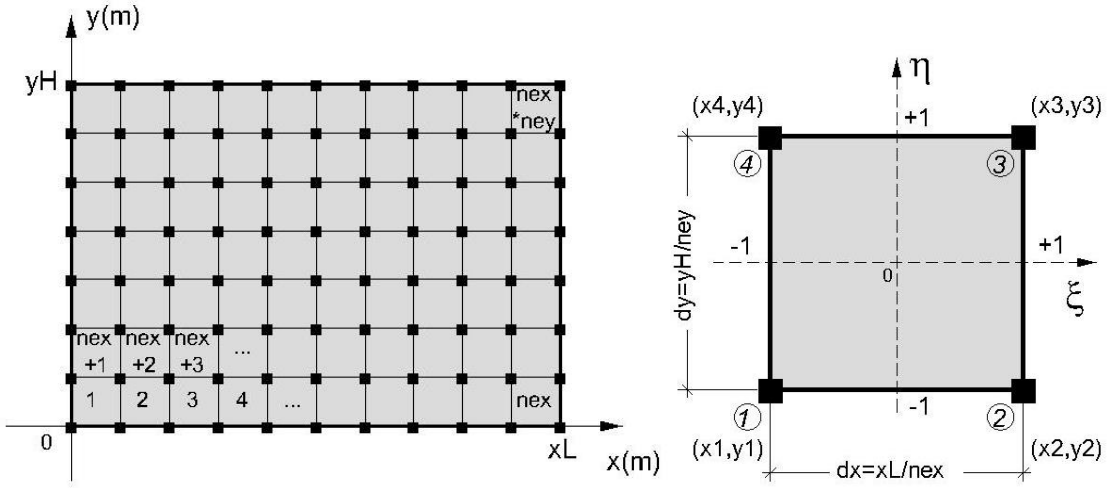

Figure 4.1: Mesh and schematic representation of the discrete fixed domain with 4-node linear rectangular elements.

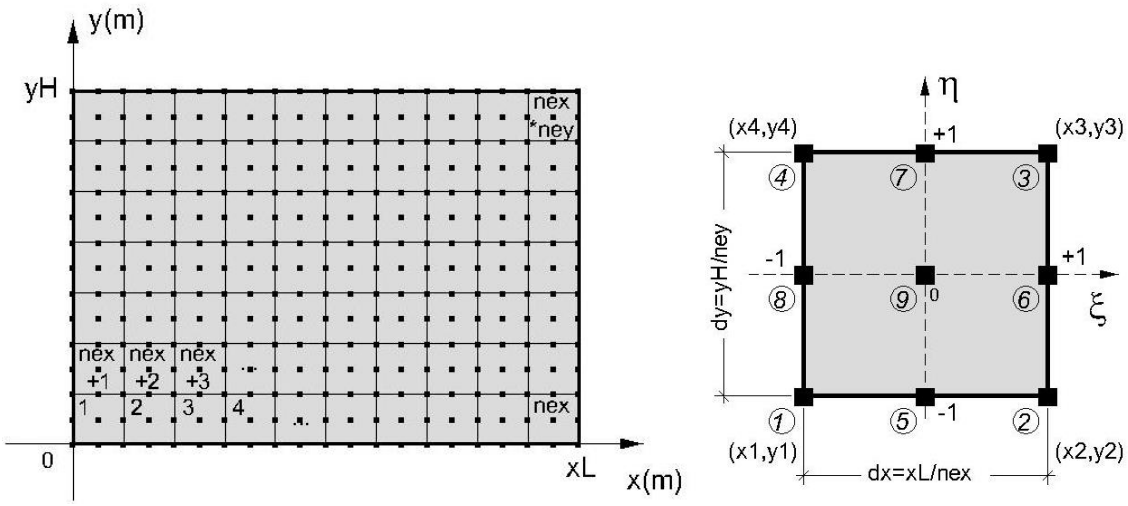

Figure 4.2: Mesh and schematic representation of the discrete fixed domain with 9-node quadratic rectangular elements.

Four-node bi-linear rectangular elements ("4L" see Figure 4.1) or 9-node bi-quadratic rectangular elements ("9Q" see Figure 4.2) are used to solve a given plane stress problem. These elements are paired in two (bi-linear or bi-quadratic) in order to define the displacement field in the horizontal (U1) and vertical direction (U2). Thus, each node has two degrees of freedom, horizontal and vertical. The element dimensions are dx (width), dy (height) and th (thickness). The stiffness matrix for these elements is calculated using an isotropic material with a unit elastic modulus E=1 Pa, a Poisson's Ratio ν, and satisfies the following relation:

$$\mathbf{f}^{e} = \mathbf{k}_0 \mathbf{u}^{e} \qquad \textbf{(41)}$$

where the element nodal displacements and forces are collected in vectors as:

- For 4-node bilinear elements $\mathbf{u}^{e}_{4\,L} = \begin{bmatrix} u_{x1} & u_{y1} & u_{x2} & u_{y2} & u_{x3} & u_{y3} & u_{x4} & u_{y4} \end{bmatrix}^{T}$, and $\mathbf{f}^{e}_{4\,L} = \begin{bmatrix} f_{x1} & f_{y1} & f_{x2} & f_{y2} & f_{x3} & f_{y3} & f_{x4} & f_{y4} \end{bmatrix}^{T}$

- For 9-node biquadratic elements $\mathbf{u}^{\mathbf{e}}_{\mathbf{9\,Q}} = \begin{bmatrix} u_{x1} & u_{y1} & u_{x2} & u_{y2} & \dots & \dots & u_{x9} & u_{y9} \end{bmatrix}^T$,

  and $\mathbf{f}^{\mathbf{e}}_{\mathbf{9\,Q}} = \begin{bmatrix} f_{x1} & f_{y1} & f_{x2} & f_{y2} & \dots & \dots & f_{x9} & f_{y9} \end{bmatrix}^T$

The stiffness matrix of an element using an isotropic material with Young's Modulus E^0 and Poisson's Ratio ν is given by:

$$\mathbf{k}_{\mathbf{e}\ mat} = E^0\ \mathbf{k_0} \qquad \textbf{(42)}$$

notice that the stiffness matrices $\mathbf{k}_{\mathbf{e}\ \mathrm{mat}}$ and $\mathbf{k_0}$ correspond to the same Poisson's Ratio ν but different Young's Modulus (E^0 and 1 Pa).

The characteristic function $\chi(\mathbf{x})$ determines which points **x** of the design domain are material points χ=1, or voids χ=0. This characteristic function is discretized with the same mesh of the finite elements, so the variables χ^e represent if the element "e" is material or void. To avoid singularity of the global stiffness matrix, the void elements are modeled as a weak phase material (Ersatz material [42]) with Young's Modulus equals to a small fraction of the Young's Modulus of the base material:

$$\chi^e = \begin{cases} 1 & \text{if material} \\ \chi_{\min} & \text{if void,} \quad (\text{e.g., } \chi_{\min} = 1e^{-6}) \end{cases} \qquad \textbf{(43)}$$
$$E^e = \chi^e E^0$$

A table of the corresponding nodes for each element is created. The global stiffness matrix (**KG)** is assembled using this table to insert the element stiffness matrix ($\chi^e E^0 \mathbf{k_0}$) of each element in the right position.

On the other hand, given the structural problem, the boundary conditions are defined by the fixed global nodal displacements ($\mathbf{U_G^{fixed}}$), the global nodal forces ($\mathbf{F_G}$) and the free degrees of freedom.

The structural equilibrium problem is reduced to a linear system of equations, and the unknown nodal displacements for the free nodes ($\mathbf{U}_G^{free}$) can be solved with:

$$\mathbf{K}_G^{free,free}\mathbf{U}_G^{free} = \mathbf{F}_G^{free} - \mathbf{K}_G^{free,fixed}\mathbf{U}_G^{fixed} \quad (44)$$

And the reaction forces for the fixed ones:

$$\mathbf{F}_G^{free} = \mathbf{K}_G^{fixed,free}\mathbf{U}_G^{free} + \mathbf{K}_G^{fixed,fixed}\mathbf{U}_G^{fixed} \quad (45)$$

As post processing process the strains, stresses, strain energy density, compliance, etc. can be obtained using the found nodal displacements ($\mathbf{U}_G$). A cantilever beam problem (see Figure 4.3) is solved using the FEA code implemented in Matlab with the following characteristics: Young's Modulus E=210GPa, Poisson's Ratio ν=0.3, load **t**=[0,-1kN], height yH=5m, width xL=8m, and thickness th=0.1m.

To validate the Matlab code, the same example is implemented in Abaqus 6.10 (FEA commercial software). The displacement fields in the horizontal (U1) and vertical (U2) directions are shown in Figure 4.4, Figure 4.5, Figure 4.6, Figure 4.7. The maximum displacement in the vertical direction is obtained at the node at which the force is applied. The maximum displacement is used to compare the results (see Figure 4.8).

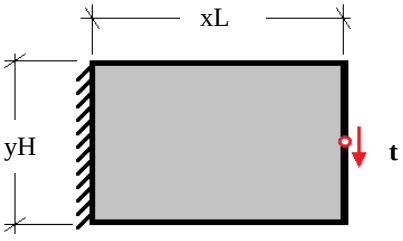

Figure 4.3: Cantilever beam problem.

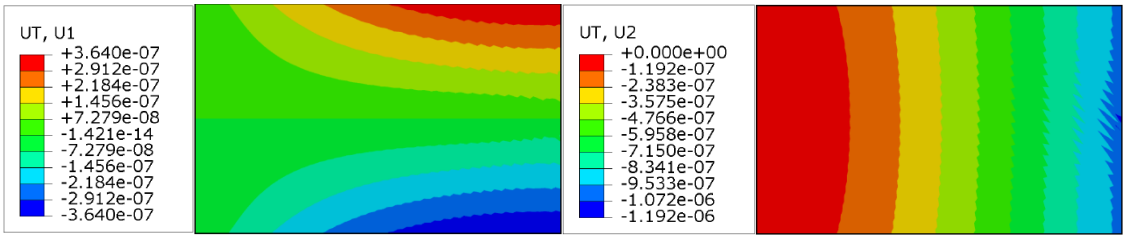

Figure 4.4: Displacements in horizontal U1 and vertical U2 direction, using Abaqus 64x40 4 node bi-linear elements.

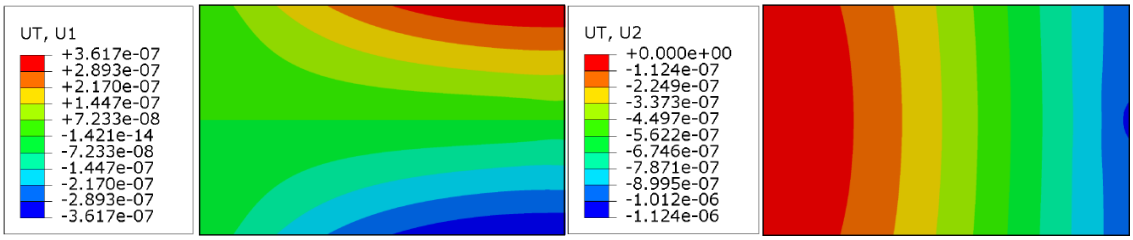

Figure 4.5: Displacements in horizontal U1 and vertical U2 direction, using Abaqus 64x40 9 node bi-quadratic elements.

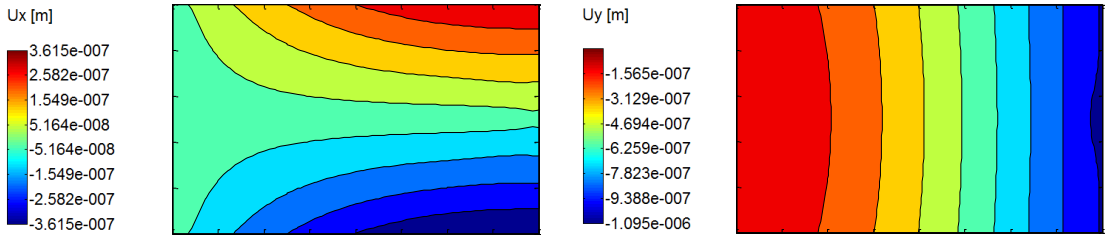

Figure 4.6: Displacements in horizontal U1 and vertical U2 direction, using Matlab 64x40 4 node bi-linear elements.

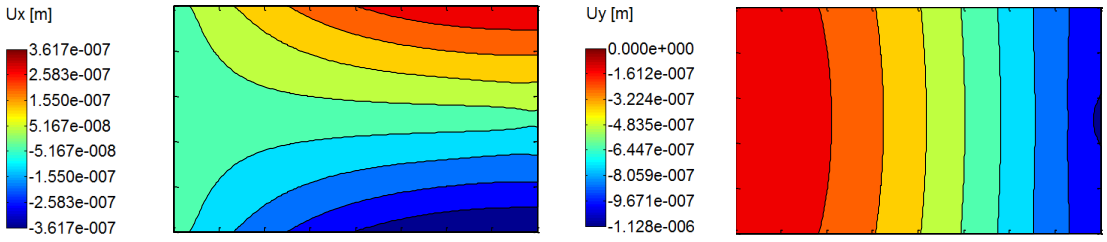

Figure 4.7: Displacements in horizontal U1 and vertical U2 direction, using Matlab 64x40 9 node bi-quadratic elements.

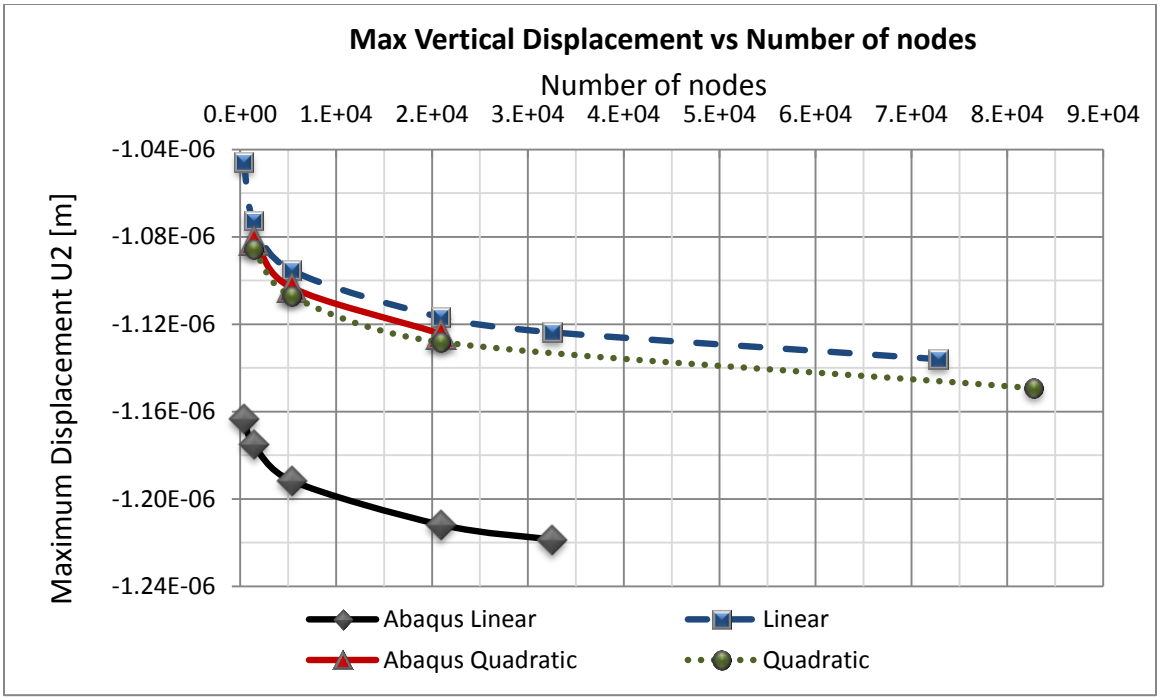

Figure 4.8: Plot of the maximum vertical displacement obtained by different element types and software.

Figure 4.4 through Figure 4.8 show that our FEA implementation in Matlab obtains similar results to the commercial software. If the number of nodes is incremented, there is a clear convergence of the results. In Figure 4.8 the Abaqus' results are truncated because the educational version of Abaqus does not allow solving problems with more than 40000 nodes. The results using Abaqus' linear element show a disagreement with respect to the others (Abaqus' quadratic elements, and our linear and quadratic elements in Matlab). Also, the displacement fields obtained using the Abaqus' linear element show non-smooth patterns (see Figure 4.4). The implementation in Matlab is validated and can be considered sufficiently accurate (error $\approx$ 0.5%).

Notice that the compliance ($c=1.16e^{-3}J$) of this problem can be obtained with the product of the external force (-1kN) with the maximum vertical displacement ($U2\approx -1.16e^{-6}m$). Any structure in this rectangular domain with less material will produce more displacement and consequently more compliance with the same loading condition. The same problem is solved for the cantilever beam with a rectangular hole in the center. The hole dimensions are a width of hx = xL/2 = 4m and a height hy = yH/2 =2.5m] (see Figure 4.9). In Matlab the hole is modeled using elements with a low Young's Modulus and in Abaqus the hole is actually void. The results for the maximum displacement in the vertical direction are shown in Figure 4.10.

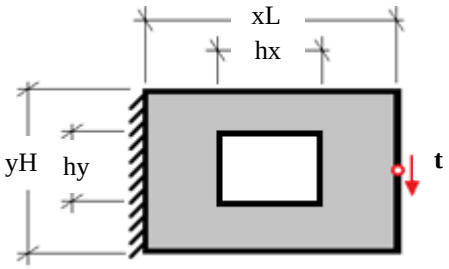

Figure 4.9: Cantilever beam problem with a rectangular hole in the center.

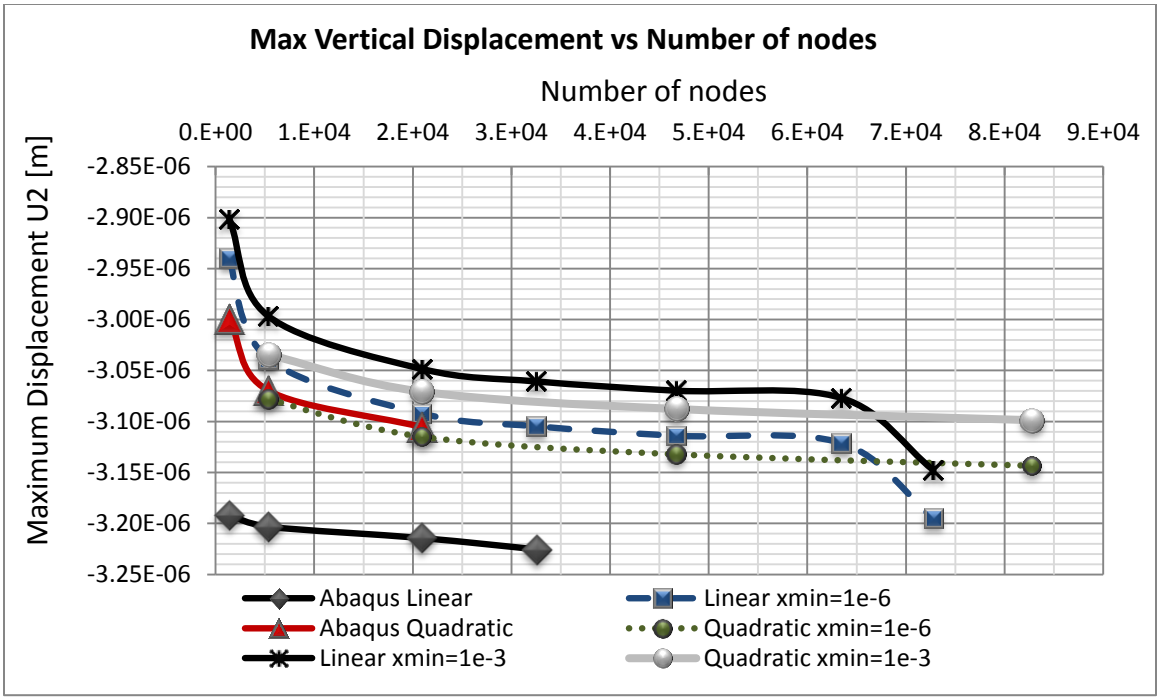

Figure 4.10: Plot of the maximum vertical displacement of a cantilever beam with a rectangular hole.

Figure 4.10 shows also that Abaqus' linear elements produce higher displacements than the quadratic elements with non-smooth displacement fields. If the void domain is modeled with smaller Young's Modulus (χmin=1e-6 instead χmin=1e-3), the maximum displacement is closer to the maximum displacement obtained by Abaqus using quadratic elements.

The use of our linear elements for the beam problem with a large number of nodes (>64000) produces a change in the convergence. Probably this error is due to the numerical computation related with the large number of "elements". For the same number of nodes more linear elements than the quadratic elements are required. However, for better modeling of the material distribution a larger number of elements is

required. The results using the quadratic elements show convergence for a larger number of nodes. Based on this preliminary analysis, linear elements with χmin=1e-6 are selected limiting the number of nodes to 50000 for a reasonable computational time.

4.2 Implemented algorithm to place a prescribed number of holes

The FEA computes the objective and its sensitivities with respect to the design variables χ^e. These design variables are updated by the two-step procedure described in section 3.4 (see Figure 4.11). First, a temporary material density distribution is obtained through the steepest descent direction ($\phi=\chi^k+\alpha\mathbf{S}$). Then, these temporary densities are penalized to a 1/0 distribution using the level set concept ($\phi\rightarrow\chi^{k+1}$). However, this technique requires choosing the value of the linear search parameter α. Since any updated configuration has a 1/0 distribution, the number of holes for the updated configuration can be counted. Thus, an algorithm to place and obtain "n_h" number of holes starting from the whole design domain full of material can be formulated as:

1) The initial configuration has the whole domain filled with material.

2) Finite element analysis of the initial configuration is executed. The objective and its sensitivities with respect to the design variables ($dL/d\chi$) are obtained.

3) Using an upper bound α_1, a new configuration can be updated (χ_1) and the number of holes (n_1) for the new configuration can be counted.

4) Using the interval halving algorithm, the lower bound (α_2) for the obtained number of holes (n_2) is computed. Configurations with n_1 number of holes can be

obtained for any α in the interval [α_1, α_2]. For example, in Figure 4.11, if $\alpha_1=\alpha_B$ then $n_1=3$ holes, and if $\alpha_2=\alpha_A$ then $n_2=2$ holes.

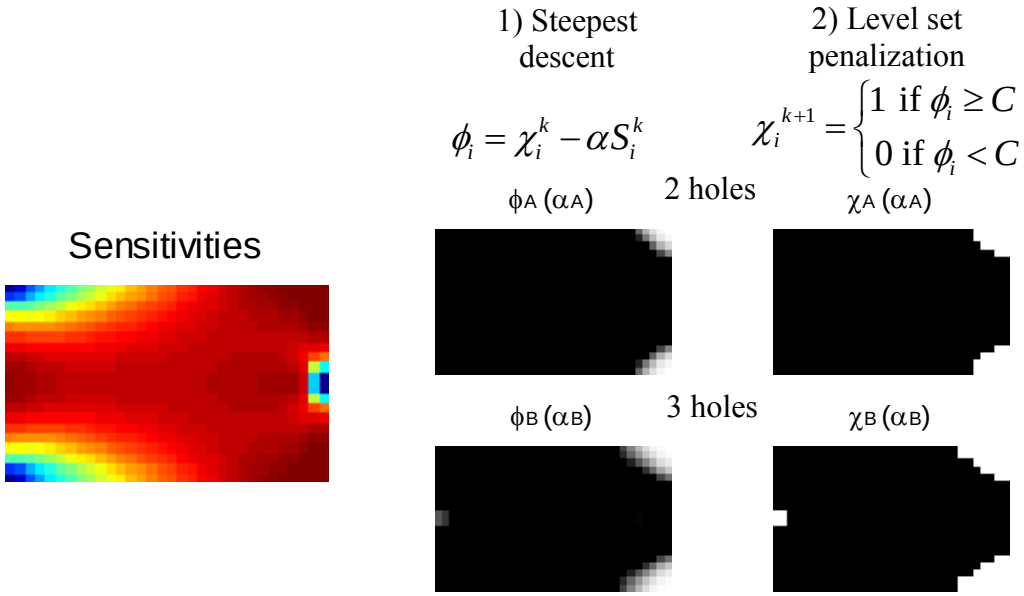

Figure 4.11 Left: Representation of the sensitivities of the full design domain. Right: Configurations obtained with the sensitivities for two different values of α.

5) Repeat step 4, using α_2 as the upper bound for the configurations with n_2 number of holes. Then, repeat again step 4 until the lower bound obtained is zero $\alpha_{lower}=0$. The intervals for the different number of holes are obtained sequentially. The limit of the lower bound is 0, where no update is produced.

6) Check if an interval for the desired n_h number of holes was obtained.

- If yes, exit

- If not, repeat the procedure from step 2 starting with a configuration of n_1 number of holes using $\alpha=(\alpha_1+ \alpha_2)/2$ to avoid unstable configurations.

The flowchart of this algorithm to obtain n_h number of holes is presented in Figure 4.12:

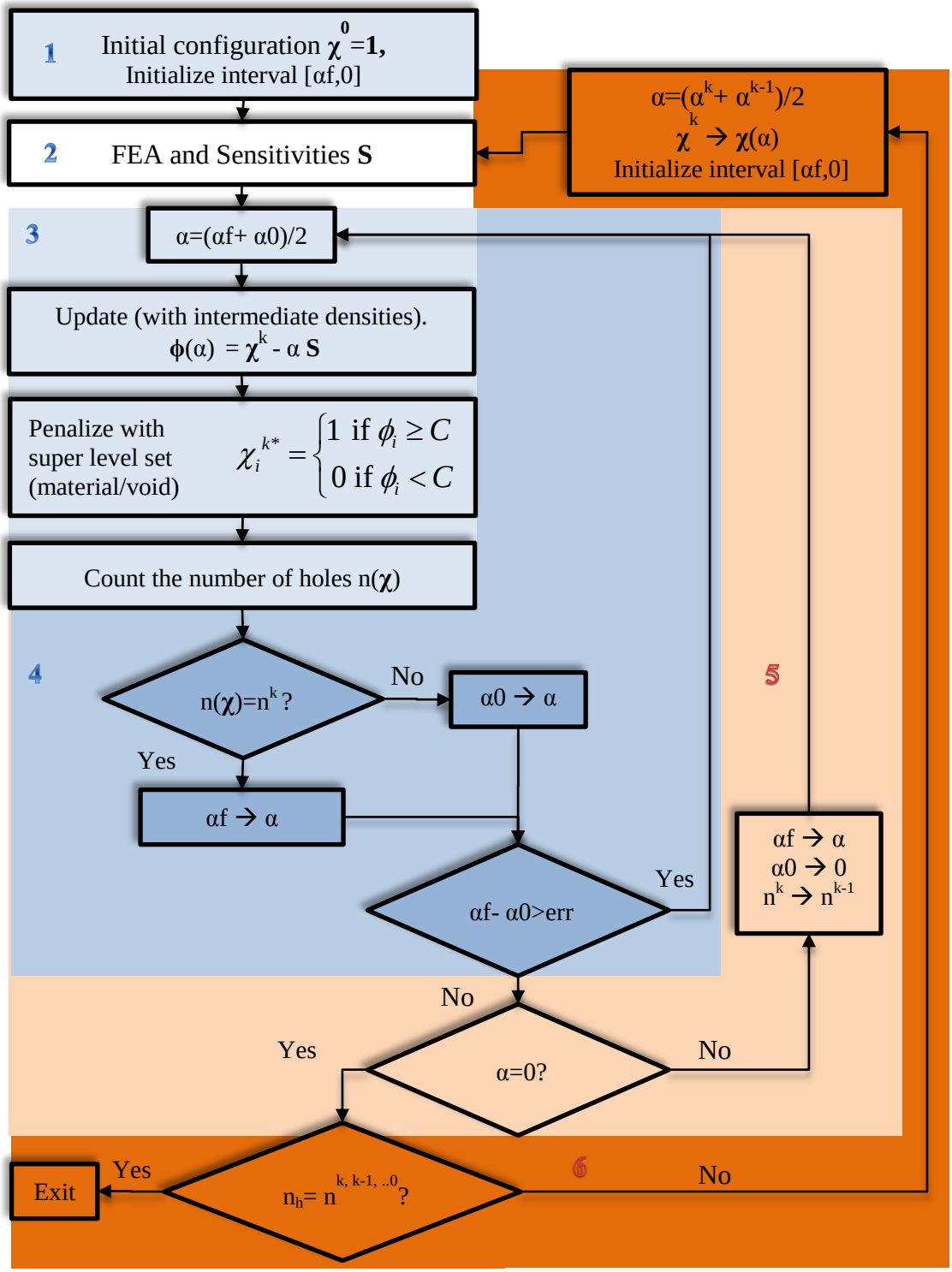

Figure 4.12: Topology optimization algorithm to obtain and place n_h holes.

4.3 Numerical examples to place n_h number of holes: minimum compliance with volume constraint problem.

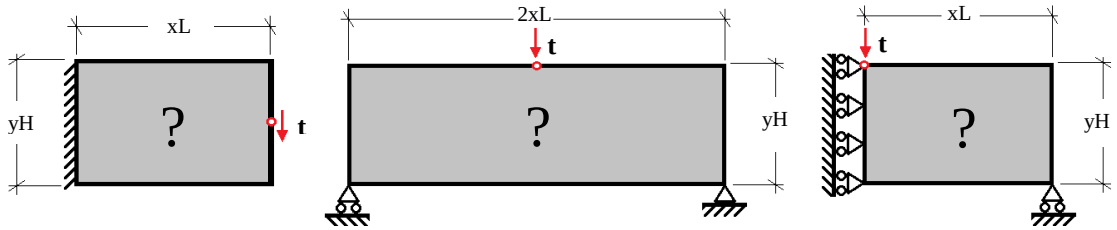

Figure 4.13 Left: Cantilever beam problem. Center: MBB-beam full domain. Right: MBB-beam half domain.

A cantilever beam problem and the called Messerschmitt-Bölkow-Blohm (MBB for the German aerospace company) beam problem (see

Figure 4.13) are treated using the algorithm to place n_h number of holes. The parameters are set as follows: Young's Modulus E=210GPa, Poisson's Ratio ν=0.3, load **t**=[0,-10kN], height yH=5m, width xL=8m, and thickness th=0.1m. The mesh size is 96 by 60 bi-linear quadratic elements (11834 nodes < limit 50000 nodes).

Figure 4.14 and Figure 4.15 show the configurations with different number of holes produced by the algorithm. The sensitivities choose which regions of material are more effective to remove with lower cost in compliance. The higher the number of holes for the configuration, the lower the volume fraction obtained. The algorithm is not able to obtain configurations with 1 or 5 holes for the cantilever beam problem, and 6 holes for the MBB-beam, because of symmetry reasons. These configurations are not optimal and in general violate the volume constraint but they represent good starting points for the shape optimization procedure explained in the next sections.

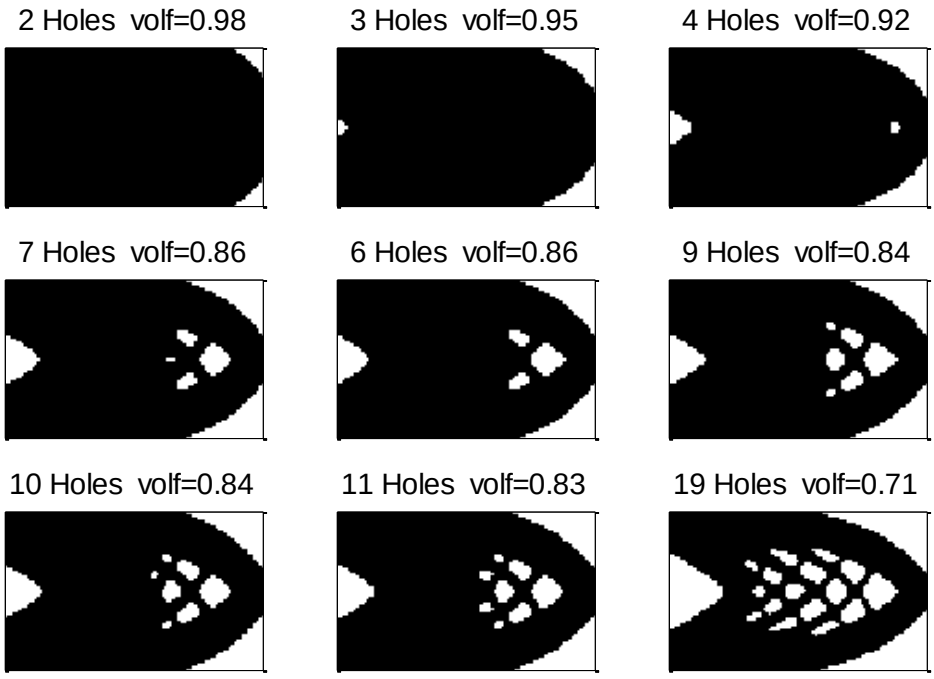

Figure 4.14: Configurations for the cantilever beam problem with different number of holes obtained by the implemented algorithm with the respective volume fraction.

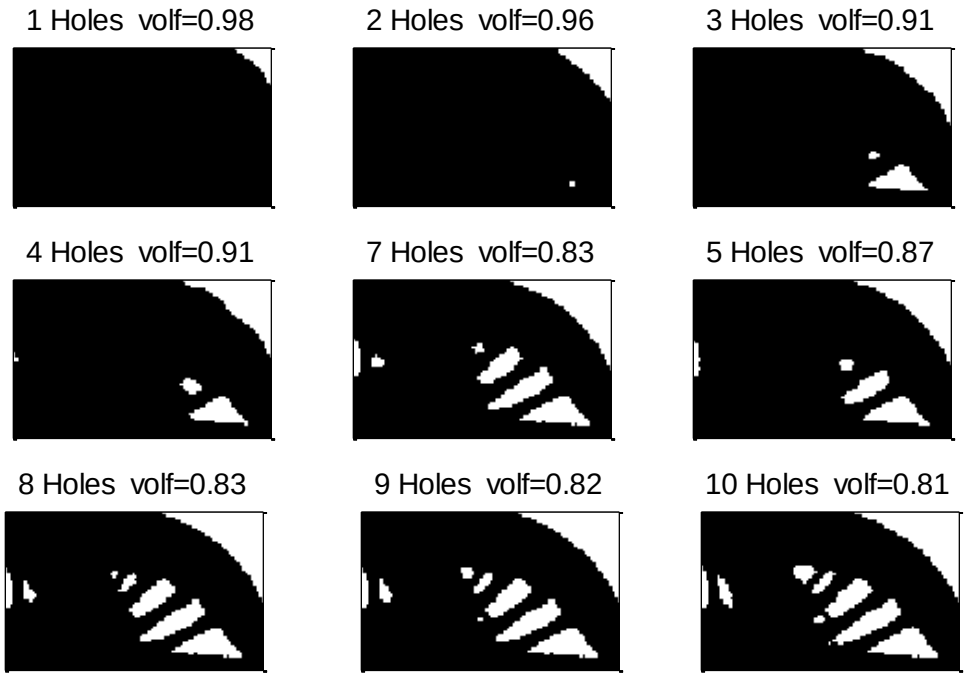

Figure 4.15: Configurations for the MBB beam problem with different number of holes obtained by the implemented algorithm with the respective volume fraction.

4.4 Boundary elements

As was discussed in the section 3.5, the elements in the material/void boundary ($\Gamma_{\mathbf{L}}$) can be conveniently identified because the material distribution is a 1/0 configuration. The norm of the gradient of the characteristic function (χ) is non-zero for the elements in the boundary:

$$\left|\nabla \chi_i\right| = \begin{cases} a & \text{if } \chi_i \in \Gamma_L \\ 0 & \text{if } \chi_i \notin \Gamma_L \end{cases} \qquad \textbf{(46)}$$

The characteristic function of the structure configuration is defined with values of either 1 or χ_{min}. Thus, forward and backward finite differences of the material densities in the horizontal and vertical direction are non-zero on the boundary $\Gamma_{\mathbf{L}}$:

$$\begin{aligned} \frac{\partial \chi_i}{\partial x}_{forward} &= \frac{\chi_{i+dx} - \chi_i}{dx} & \frac{\partial \chi_i}{\partial x}_{backward} &= \frac{\chi_i - \chi_{i-dx}}{dx} \\ \frac{\partial \chi_i}{\partial y}_{forward} &= \frac{\chi_{i+dy} - \chi_i}{dy} & \frac{\partial \chi_i}{\partial y}_{backward} &= \frac{\chi_i - \chi_{i-dy}}{dy} \end{aligned} \qquad \textbf{(47)}$$

χ_{i+dx}, χ_{i-dx}, χ_{i+dy} and χ_{i-dy} are the densities of the neighbor elements of the "ith" element. Also, dx and dy are the element sizes in the horizontal and vertical direction respectively. The numerical norm of the gradient obtained is:

$$\left|\nabla \chi_i\right| = \frac{1}{2}\sqrt{\left(\left|\frac{\partial \chi_i}{\partial x}_{forward}\right| + \left|\frac{\partial \chi_i}{\partial x}_{backward}\right|\right)^2 + \left(\left|\frac{\partial \chi_i}{\partial y}_{forward}\right| + \left|\frac{\partial \chi_i}{\partial y}_{backward}\right|\right)^2} \qquad \textbf{(48)}$$

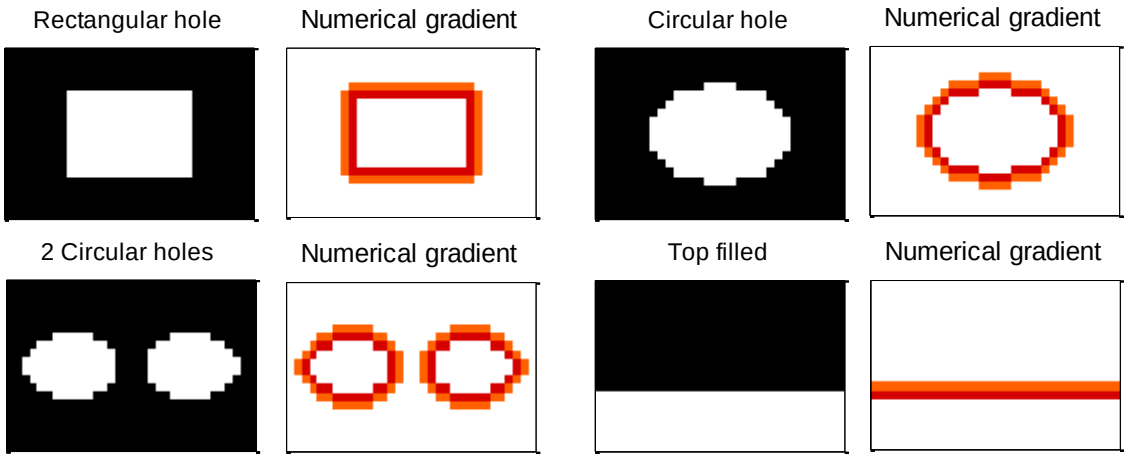

Figure 4.16: Visual representation examples of the numerical gradient. Two boundary elements: orange elements from the material boundary, red elements from the void boundary.

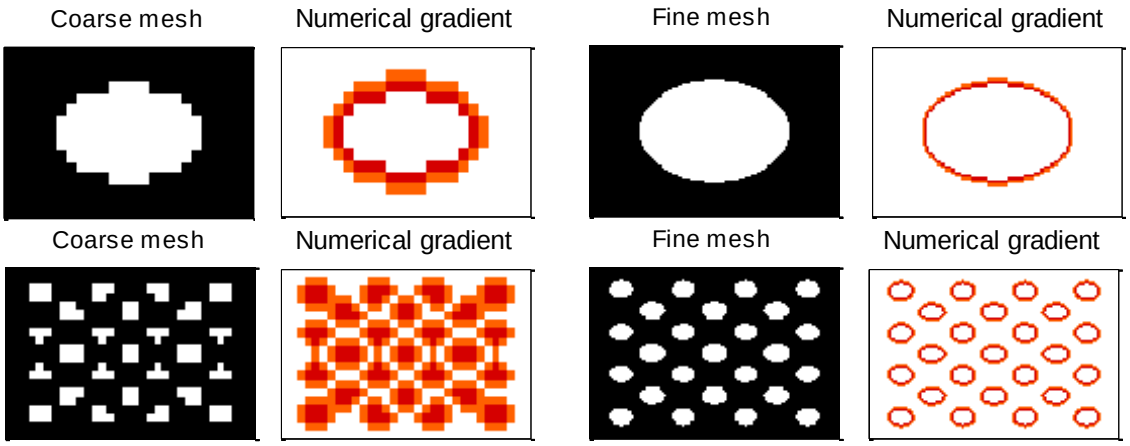

Figure 4.17: Visual representation examples to compare the effect of the mesh in the resolution of the topology and the boundary.

In Figure 4.16, the material/void boundaries are identified for different topologies. Since the boundary is the transition between the material and the void in the design domain, two layers of elements are obtained: one in the material domain, and one in the void domain. A finer mesh will obviously result in thinner layers (see Figure 4.16 and Figure 4.17).

4.5 Shape optimization

Using the numerical gradient implemented in the previous section, all the elements that have a non-zero gradient are part of the material/void boundary. If the elements of this boundary are added or removed, the boundary will change but the number of holes will remain the same (exceptions are discussed in section 3.5 see Figure 3.4). Shape optimization is like topology optimization considering as design variables only the densities of the boundary elements. Only these densities of the elements of the boundary are updated.

The boundary design variables (χ_b) can be updated with the same technique presented in 3.4 selecting α to add/remove a certain amount of material dV. The volume dV should be small and can be chosen constant in the optimization process. However, if the volume constraint is active, dV is negative (remove material) and if the volume constraint is inactive, dV is positive. The sign changes because the Lagrange multiplier of the volume constraint is zero if the volume constraint is inactive. In the iterative process, once the volume fraction is close to the volume constraint and no improvement in the compliance is obtained the material added/removed dV is reduced in order to achieve convergence.

If the volume constraint is active, the sensitivities must be positive to remove material using the steepest descent method. To ensure this, the Lagrange multiplier of the volume constraint is estimated as follows:

$$\frac{dL}{d\chi_i} = S_i^k = -\mathbf{u_i}^T \mathbf{k_0} \mathbf{u_i} + \frac{\lambda}{N} \qquad \text{Sensitivities} \qquad (49)$$

$$\lambda = N \max\left(\mathbf{u_i}^T \mathbf{k_0} \mathbf{u_i}\right) \quad (50)$$

If the volume constraint is inactive the Lagrange multiplier of the volume constraint is zero $\lambda = 0$.

A flowchart of the update algorithm that adds/removes an amount of volume dV is presented:

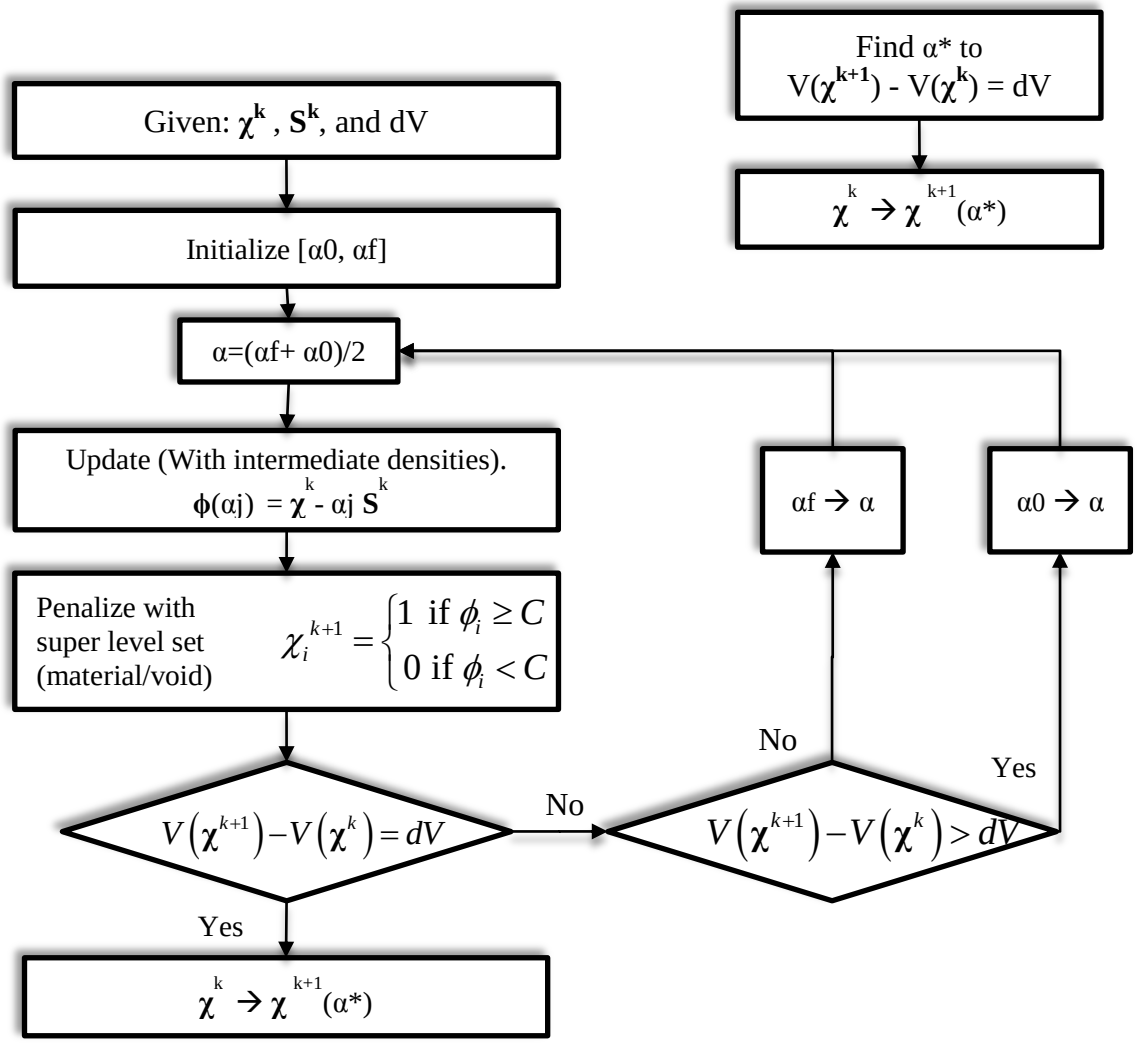

Figure 4.18 Left: Detail algorithm for the update of the material void distribution adding/removing an amount of volume dV with level set penalization. Right: non-detail algorithm.

A flowchart for the overall shape optimization algorithm is shown:

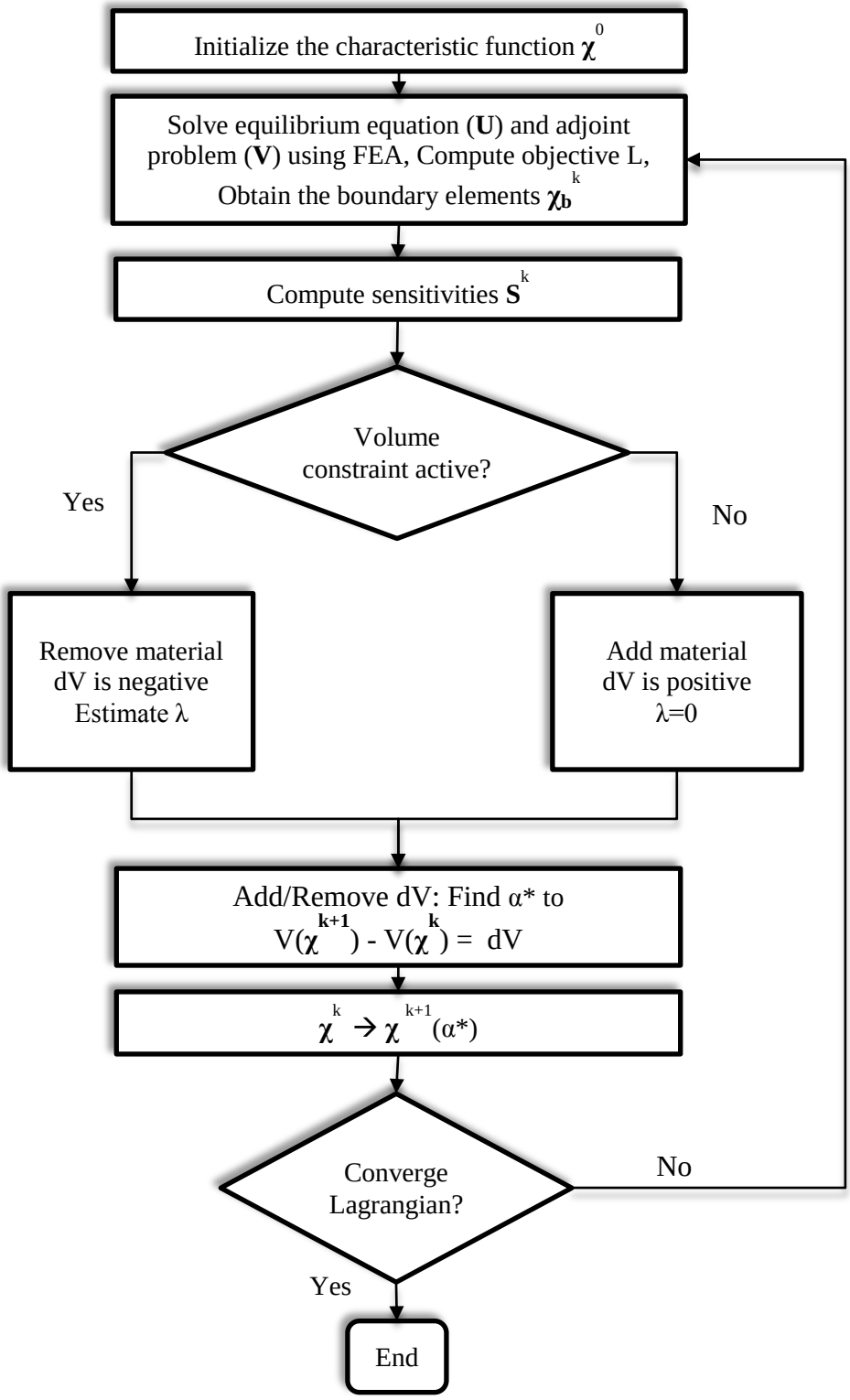

Figure 4.19: Algorithm for shape optimization.

4.6 Shape optimization numerical examples: minimum compliance with volume constraint problem.

The minimum compliance with a volume constraint for the cantilever beam problem described in section 4.3 is solved using the shape optimization algorithm. A 80 by 50 element mesh is used. Initial configurations with holes located in different places are used to show the effectiveness of the shape optimization process. The constraint on the volume fraction is 0.3 and the volume fraction removed is kept constant in each iteration with dV=1%. The convergence criteria used in the Lagrangian is 5e-4% for the last 6 configurations. Optimal shapes are obtained at the end of the process when convergence is achieved. Starting with three and six holes, the optimization history is shown for the Lagrangian, the compliance, and the volume constraint for the cantilever beam problem in the following figures 4.20 to 4.23:

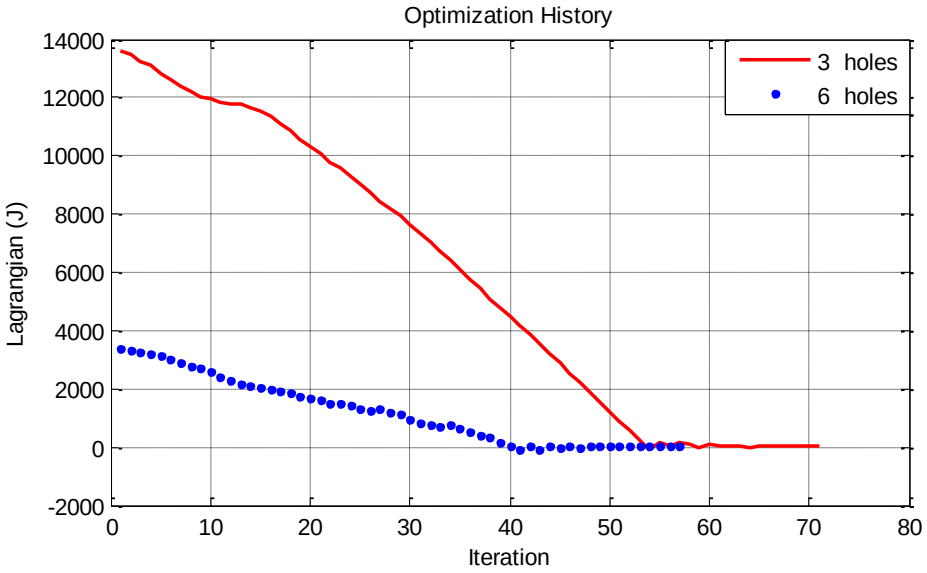

Figure 4.20: Optimization history of the Lagrangian for the cantilever beam problem with an initial configuration of three and six holes

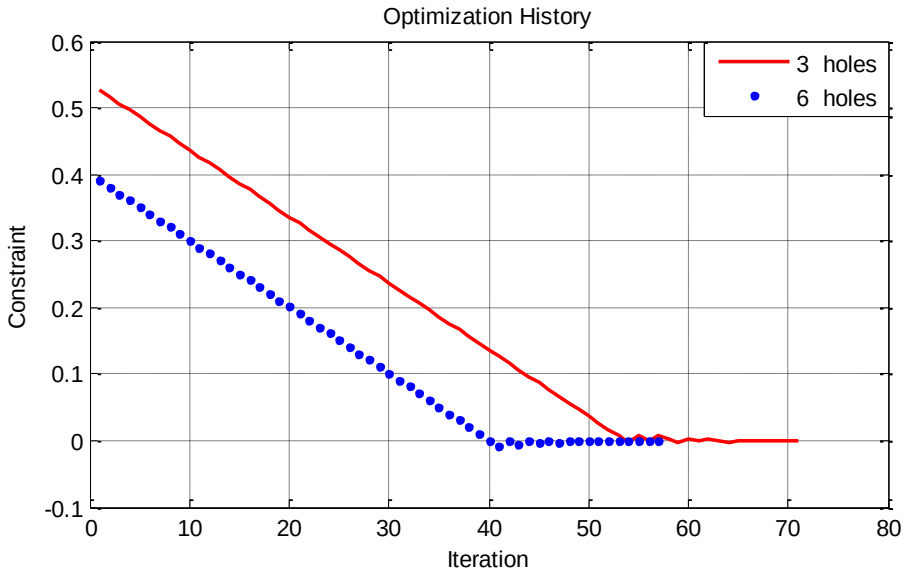

Figure 4.21: Optimization history of the volume constraint for the cantilever beam problem with an initial configuration of three and six holes

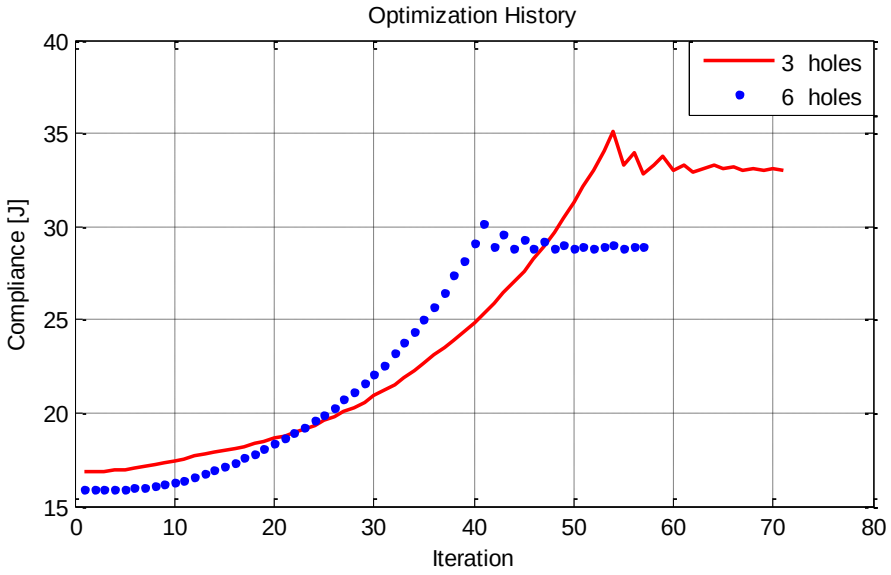

Figure 4.22: Optimization history of the compliance for the cantilever beam problem with an initial configuration of three and six holes

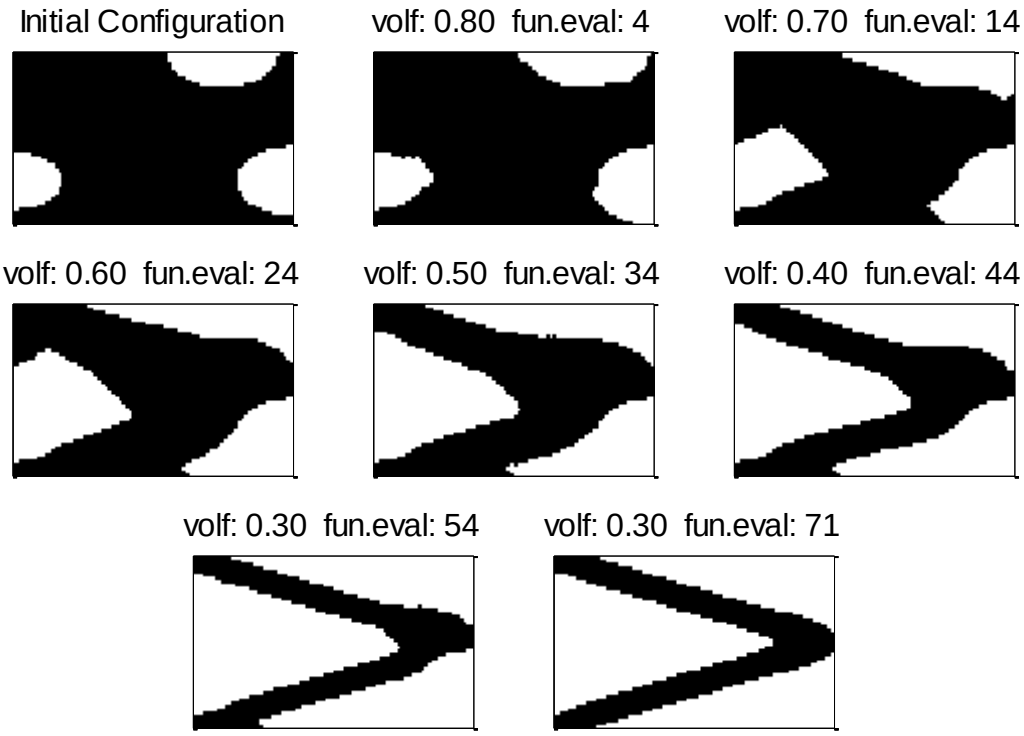

Figure 4.23: Initial configuration with three holes (volume fraction 0.83), configurations obtained in the shape optimization process, and optimal configuration for the cantilever beam problem.

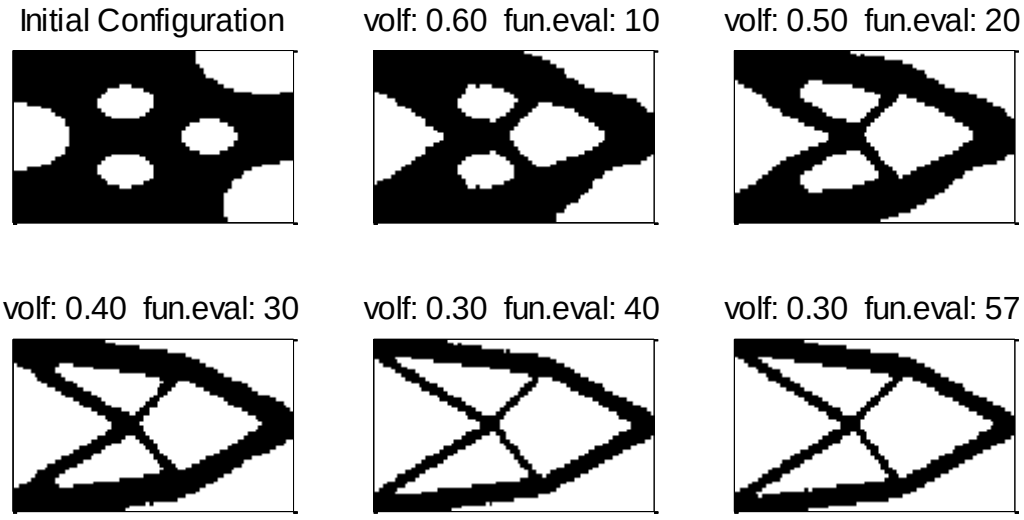

Figure 4.24: Initial configuration with six holes (volume fraction 0.70), configurations obtained in the shape optimization process, and optimal configuration for the cantilever beam problem.

This procedure of shape optimization changes the size and shape of the holes. Also, the location of the holes can be calibrated. The number of holes can be maintained easily unless two boundaries merge. The sensitivities determine which elements of the material boundary should be removed, and which elements of the void boundary should be added. The convergence of the Lagrangian when adding/removing material (dV) implies that the elements added at certain volume are again removed to obtain the same volume.

4.7 Minimum compliance with volume and the number of holes constrained

The topology optimization problem for minimum compliance with constrained volume and number of holes is solved in two main steps.

- First, starting form a full solid plate, the topology optimizer will obtain the first configuration with n_h holes removing iteratively the material as was presented and explained in sections 4.2 and 4.3. At this point the topology satisfies the constraint on the number of holes.
- Second, shape optimization is carried out, maintaining the number of holes as explained in sections 4.5 and 4.6.

The following figures show the results for the cantilever beam problem. Optimal topologies for various volume fractions and various numbers of holes are obtained. The characteristics of the problems are the same as the problems in section 4.3. A mesh with 96 by 60 elements is used.

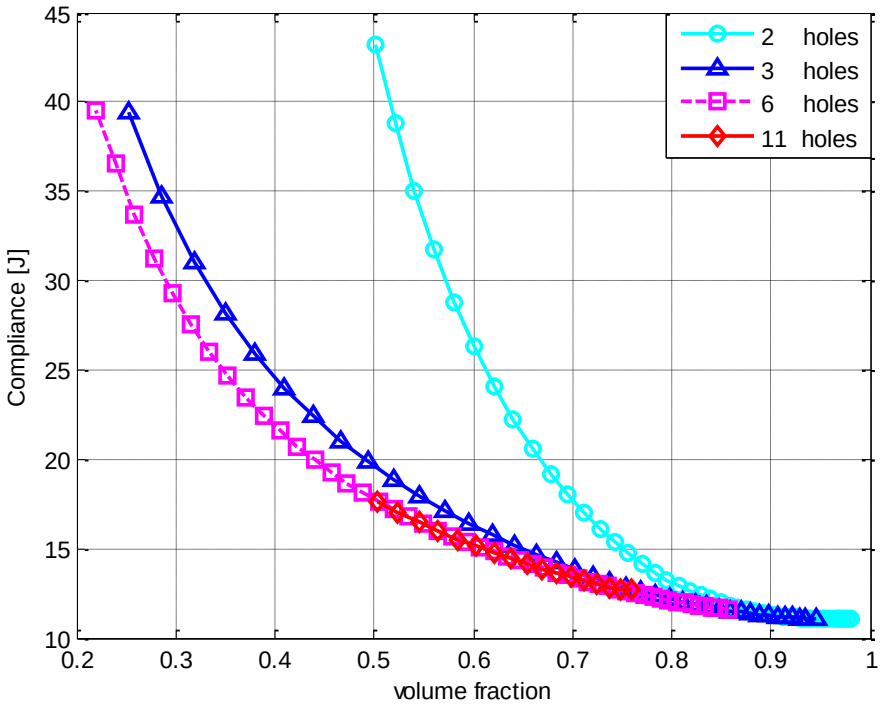

Figure 4.25: Optimal compliance vs. volume fraction constraint obtained for the cantilever beam problem with controlled number of holes.

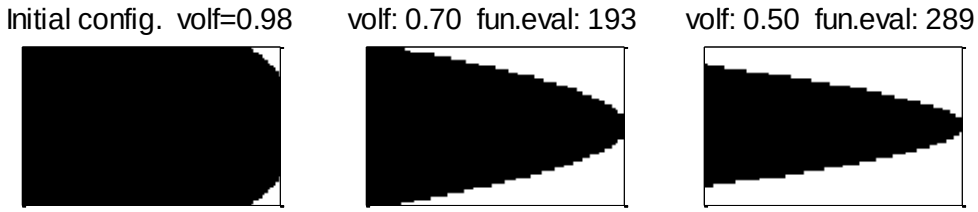

Figure 4.26: Optimal design configurations obtained for the cantilever beam problem with 2 holes.

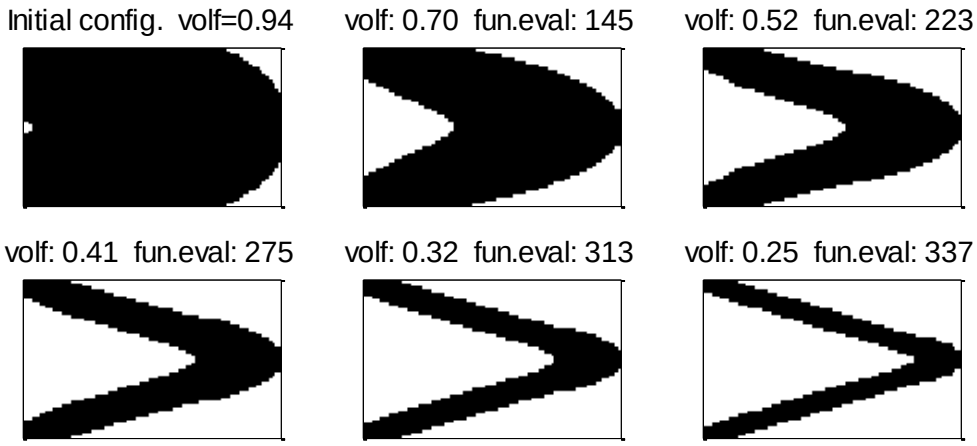

Figure 4.27: Optimal design configurations obtained for the cantilever beam problem with 3 holes.

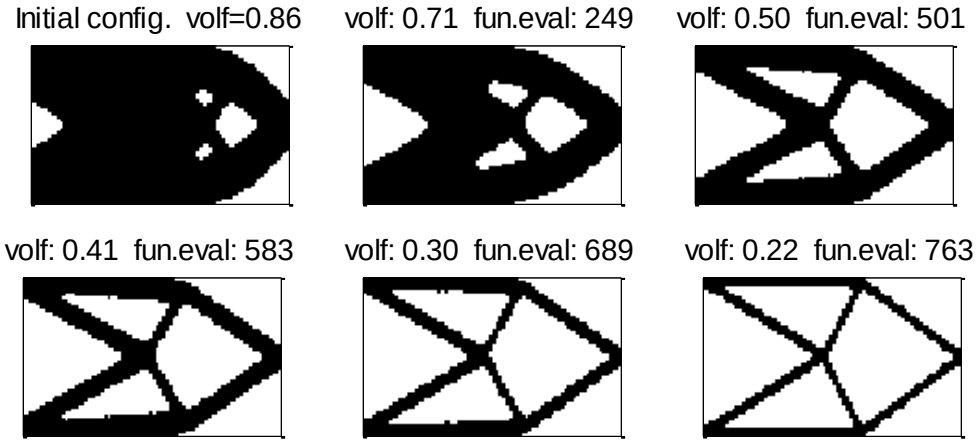

Figure 4.28: Optimal design configurations obtained for the cantilever beam problem with 6 holes.

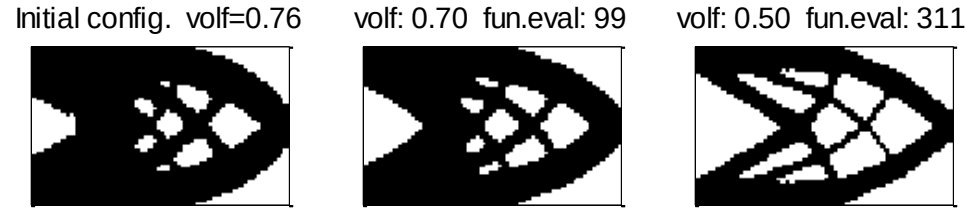

Figure 4.29: Optimal design configurations obtained for the cantilever beam problem with 11 holes.

Figure 4.25 through Figure 4.29 show that the proposed algorithm improves the Lagrangian while the number of holes is fixed according to ensure manufacturing constraints. Notice that optimal configurations with more holes at the same volume constraint have lower compliance. However, this difference is not always very significant. For the cantilever beam problem, Figure 4.25, the curve of 2 holes differs from the others for volume fractions below 0.85. The advantage of having more than 2 holes is important for volume fractions below 0.85. The curves of 3, 6, and 11 holes are very close, that means that it is no worth increasing the complexity of the solution since the advantage in terms of compliance is relatively small. The following figures show the results for the MBB-beam problem.

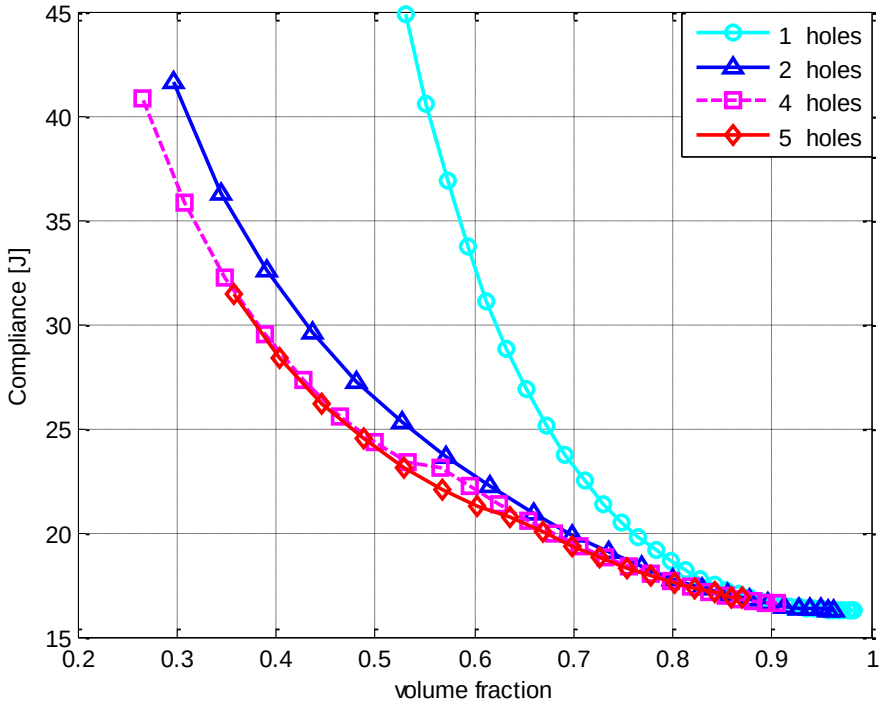

Figure 4.30: Optimal compliance vs volume fraction constraint obtained for the MBB-beam problem with number of holes controlled.

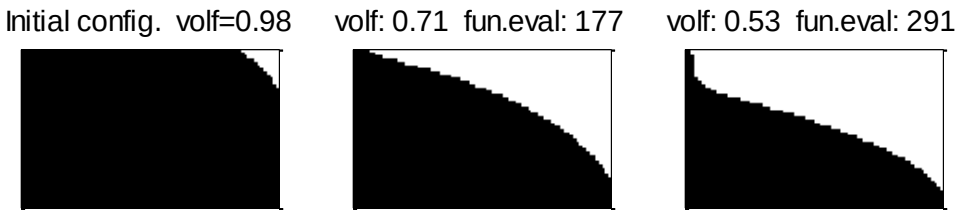

Figure 4.31: Optimal design configurations obtained for the MBB-beam problem with 1 holes.

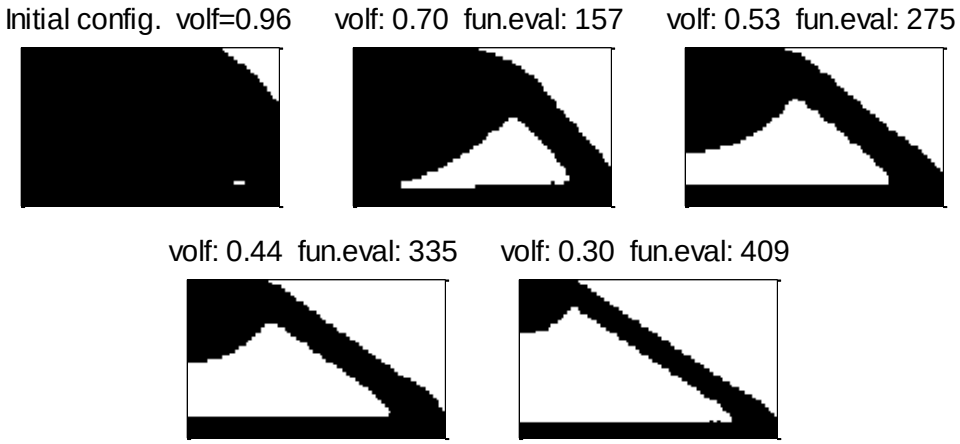

Figure 4.32: Optimal design configurations obtained for the MBB-beam problem with 2 holes.

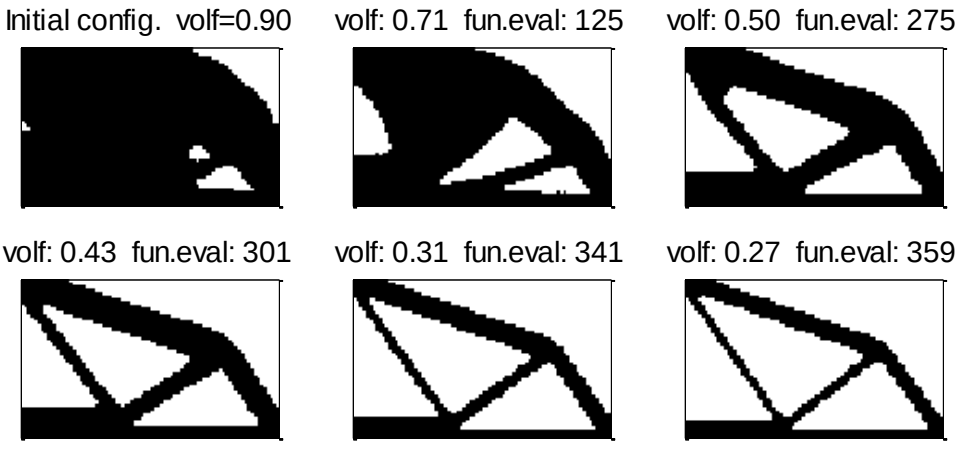

Figure 4.33: Optimal design configurations obtained for the MBB-beam problem with 4 holes.

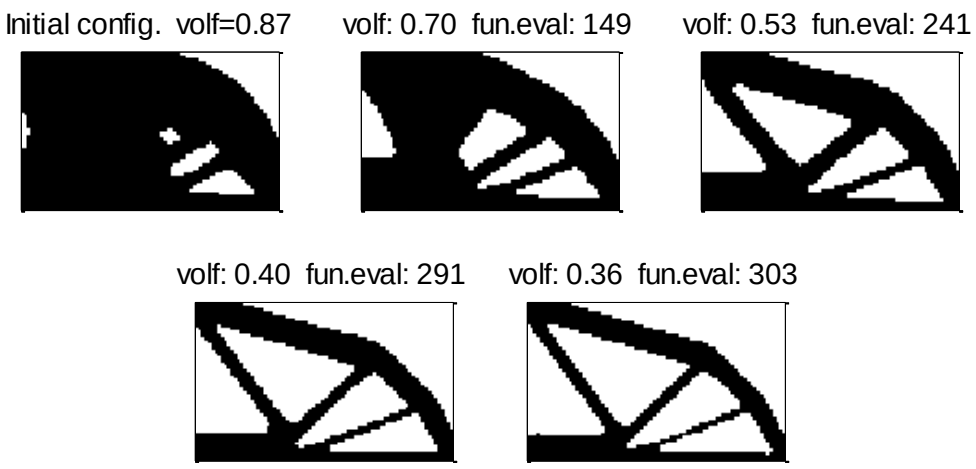

Figure 4.34: Optimal design configurations obtained for the MBB-beam problem with 5 holes.

For the MBB-beam problem, Figure 4.30 through Figure 4.34, similarly to the cantilever beam problem, optima,l topologies with the desired number of holes were obtained. For low volume fraction a high number of holes is difficult to maintain because of boundary merge.

4.8 Comparison with the literature

The problem solved in this work for the cantilever beam with a volume constraint of 0.4 is similar as the one solved by Belytschko et al. (Young modulus is 1000Pa, thickness of the plate is 0.2m and the load is 1N, solution shown in Figure 4.36 [45]) and Yamada et al. (Poisson's Ration of 0.31 and load is not specified, solutions shown in Figure 4.36 [4]), however the optimal material distribution must be the same because the structural problem is linear. Position, shape, and size of these holes in the optimal configurations obtained are quite similar to the ones reported in the literature as shown in the following figures:

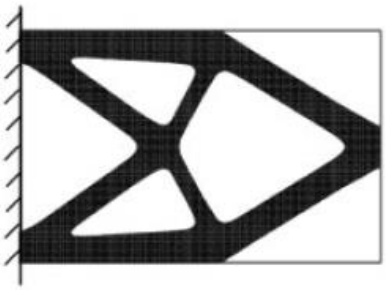

Figure 4.35: Optimal configurations for the cantilever beam by Belytschko et al. [45] for a volume constraint of 0.4.

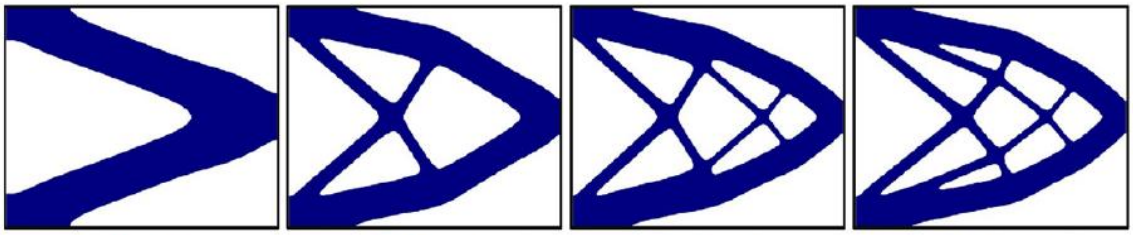

Figure 4.36: Optimal configurations for the cantilever beam by Yamada et al. [4] for a volume constraint of 0.4 with different parameter a) τ=5e-4, 3 holes, b) τ=5e-5, 6 holes, c) τ=3e-5, 9 holes, and d) τ=2e-5, 11 holes.

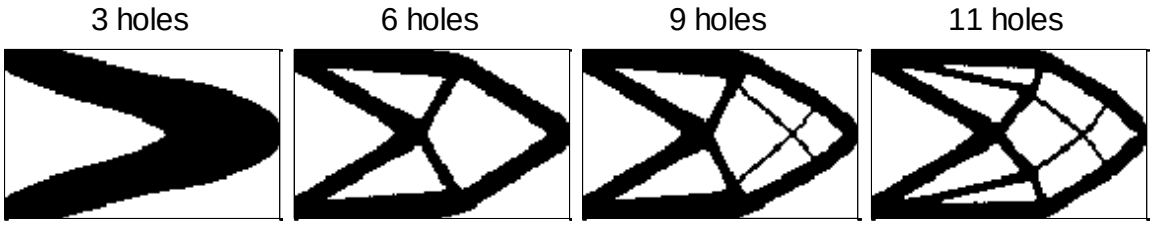

Figure 4.37: Optimal configurations for the cantilever beam by our method for a volume constraint of 0.4 (mesh 128x80).

The configuration with 6 holes obtained by us is exactly the same one reported by Belytschko. However, there is some difference of our configurations compared for the one reported by Yamada using the different parameters τ.

For a quantitative comparison, the SIMP method is implemented with the same characteristics as our problem. Modifying Sigmund's 99 line Matlab code [72] to solve

the cantilever beam problem for a volume constraint of 0.4, the following results are obtained:

Figure 4.38: Optimal configurations for the cantilever beam by SIMP for a volume constraint of 0.4 with different the filter parameter a) rmin=2 (6 holes) b) rmin=1 (198 holes) (mesh 128x80).

Our optimal configuration with 6 holes is exactly the same as the one obtained by the SIMP method with the filter parameter rmin=2. Also, this configuration is the same as the one reported by Belytschko. In the following table, the compliance of the optimal configurations obtained is shown:

Table 4.1: Compliance of the optimal configurations.

Number of holes	3	6	9	11	198
Compliance by SIMP (J)	-	22.366	-	-	22.125
Compliance by our method (J)	24.396	21.549	21.470	21.190	-

The results obtained by our method compared with the ones obtained by SIMP show better values of compliance (see Table 4.1). Also, it can be notice that more number of holes results in lower compliance.

4.9 Summary

In this chapter, the algorithms of the procedure to place a prescribed number of holes and do shape optimization was presented. The implementation in Matlab of the

methods proposed in this work was explained. Example problems for topology optimization problems for minimum compliance with constrained volume and number of holes are solved. This method shows numerical stable solutions and was validated by comparing the results with the ones obtained by the literature. In the next chapter, the concluding remarks and the future work is presented.

CHAPTER FIVE: CONCLUDING REMARKS

Several research questions were posed at the beginning of this work. This chapter restates them then shows how they were addressed and what conclusions were obtained. The main question was:

Is it possible to formulate a topology optimization problem with a constraint on the number of holes?

This question was then decomposed into:

a. If so, can a method be constructed to obtain the solution?
    i. How can the number of holes be controlled in the optimization process?
    ii. Can a gradient descent method be used in the algorithm to obtain optimal solutions?
b. Does the problem have a numerically stable solution?
c. Is it possible to prove local optimality? Are the position, shape, and size of these holes in the solution local optimum?

the answer to the main question is yes. In order to achieve that goal, the topology optimization problem was reformulated by dividing it into three sequential sub-problems:

1) Defining the number of holes.
2) Locating the holes.
3) Obtaining the optimal shape and size of the holes.

The number of holes is imposed as a constraint of the optimization problem and is defined by the designer and obviously by the complexity level desired for the solution.

a. The method constructed to solve the topology optimization problem with a constraint on the number of holes, first locates the number of holes and subsequently obtains their optimal shapes and sizes.

   To locate the number of holes improving the objective and the constraints of the problem, the topology optimization problem is formulated using Lagrange relaxation where the other constraints are included in the objective by the use of Lagrange multipliers. The process should generate the prescribed number of holes, and then keep the number of holes fixed.

      i. To control the number of holes every configuration obtained in the optimization process consist of elements that either have or do not have material. The number of holes and the boundaries are well defined for a material/void (1/0) configuration without intermediate densities. Starting from a full-design domain, updated configurations with certain number of holes are obtained, although not necessarily the number of holes desired. So, the update process is repeated starting from the last configuration until the prescribed number of holes is obtained.

      Once the constraint on the number of holes is satisfied and the holes are practically well located, only the size and the shape of these holes must be changed. If only the elements that belong to the boundaries can be added/removed, changes on the boundaries are allowed without the creation of new holes. The update configuration has also a 1/0 distribution, and the procedure is repeated by changing the shape and

the size of the holes towards the optimal configuration. Thus, in this shape optimization process the number of holes is fixed but the objective minimized in an iterative process.

ii. In a discrete domain, the gradient of the Lagrangian with respect to the densities represents how the Lagrangian changes with respect to the change of the densities in each element. The information of this gradient is vital because it shows which elements can reduce the Lagrangian the most. The gradient descent method updates the densities but the new configuration has intermediate densities. Thus, the level set concept is used to penalize the intermediate densities towards a 1/0 configuration. Densities above or equal to a threshold C are updated as material and densities below that threshold are voids. Thus, the elements with significant gradient values will effectively change the element from material to void or vice versa. In this way, since the elements that reduce the Lagrangian the most change, the Lagrangian should decrease for the new configuration. This cannot be justified analytically; just numerical convergence of the implementation can prove the effectiveness of the method.

b. The topology optimization problem to minimize the compliance with a constraint on the volume and number of holes for a cantilever beam problem and MBB beam problem have numerically stable solutions. Examples of these solutions are shown in Chapter Four. Also, the use of a sensitivity filter

that smoothens the distribution of the sensitivities helps eliminate numerical instabilities that are due to the FEA discretization. Numerical instabilities such as checkerboards as well as mesh dependency have not occurred in the configurations. Each void element in a checkerboard pattern is a hole in the method presented, so the method itself deals with the checkerboard patterns by the use of the sensitivity filter and the constraint on the number of holes.

c. Local optimality for the topology optimization problem for minimum compliance with a constraint on the volume is not proven analytically in this work.

On the other hand, the convergence of the algorithms proposed is evidence that local optimal solution is achieved. If the constraints of the problem, including the constraint on the number of holes, are satisfied and no further improvement on the objective is produced, convergence is achieved. Position, shape, and size of these holes in the optimal configurations obtained are similar to the ones reported in the literature showing evidence that the solution obtained is a local optimum.

5.2 Contributions

The list of contributions to the engineering community in this work includes:

- A methodology to solve the topology optimization problem with a constraint on the number of holes.

- Topology optimization divided and formulated in three subsequent sub-problems: number of holes, location of the holes and optimal size and shape of the holes.
- Justification of the use of the level set penalization for obtaining 1/0 configuration in order to define properly the holes and their boundaries.
- Shape optimization process that updates the elements in the boundary using the same procedure as the topology optimization update.

5.3 Future work

The method to obtain optimal topologies with a constraint on the number of holes presented in this work is general, but it was implemented just for minimum compliance with volume constraint problems. There are several areas in which this research could be further explored.

5.3.1 Prove local optimality for 1/0 configuration

Local optimality can be proven if intermediate densities are allowed with the satisfaction of the KKT conditions. However, the optimal configuration must have a 1/0 material distribution and the constraint on the number of holes must be included also in the KKT conditions. Thus, a further explanation and exploration of the local optimality conditions including the constraint on the densities to 1/0 configurations and the constraint on the number of holes should be done.

5.3.2 Different objectives and constraints

This method for topology optimization with a constraint on the number of holes should be implemented for different objectives and constraints. Also, examples should be solved to show the strength of the method. Potential problems that can be solved are: compliant mechanisms, vibrations, thermal problems, maximum stress problems, etc.

5.3.3 Three dimensions space problems

Major industrial applications involve 3D problems. The extension of this method from a 2D problem to 3D should not face major hurdles, and implementations and examples of 3D problems should be addressed.

5.3.4 Multi-material topology optimization

In this work, optimal material/void distribution is obtained for a constraint number of holes. This method can be extended to solve multi-material topology optimization problems. Constraints on the number of holes for each material can be imposed and/or constraints on the number of the instances of each material can be prescribed.

REFERENCES

[1] Bendsoe M., Kikuchi N., "Generating optimal topologies in structural design using a homogenization method," *Computer methods in applied mechanics and engineering,* vol. 71, pp. 197-224, 1988.

[2] Bendsoe M., Sigmund O., Topology optimization: theory, methods and applications., Berlin: Springer, 2003.

[3] Haber R., Jog C., Bendsoe M., "A new approach to variable-topology shape design using a constraint on perimeter," *Structural and Multidisciplinary Optimization,* vol. 11, no. 12, pp. 1-12, 1996.

[4] Yamada T., Izui K.,Nishiwaki S., Takezawa A., "A topology optimization method based on the level set method incorporating a fictitous interface energy.," *Comput. Methods Appl. Mech. Engrg.,* vol. 199, no. 45-48, pp. 2876-2891, 2010.

[5] Luo J., Luo Z., Chen S., Tong L., Wang M., "A new level set method for systematic design of hinge-free compliant mechanisms," *Computer methods in applied mechanics and engineering,* vol. 198, pp. 318-331, 2008.

[6] Chen S., Wang M., Liu A., "Shape feature control in structural topology optimization," *Computer-Aided design ,* vol. 40, pp. 951-962, 2008.

[7] Pahl G., Beitz W., Feldhusen J., Grote K., Engineering Design: A systematic approach., London: Springer, 2007.

[8] Vanderplaats G., Numerical optimization techniques for engineering design., Santa Barbara: McGraw-Hill, 1984.

[9] Leiva J. P., "Topometry optimization: Anew capability to perform element by element sizing optimization of structures," in *10th AIAA/ISSMO Multidisciplinary Analysis and Optimization Conference. Multidisciplinary Analysis Optimization Conferences*, New York, 2004.

[10] Sen A., Londhe A., "Application of topology and topography optimization in design of engine FEAD brackets and covers," in *Altair CAE users conference: Innovation through simulation*, Bangalore, 2006.

[11] Michell AGM, "The limits in economy of materials in frame structures," *Philosophical magazine,* vol. 8, no. 47, pp. 589-597, 1904.

[12] Prager W, "Optimality criteria derived from classical extremum principles," *SM studies series, solid mechanics division, University of Waterloo, Ontario/CANADA,* 1969.

[13] Prager W, "A note on discretized Michell structures," *Comput. Meth. Appl. Mech. Eng.*, vol. 3, pp. 349-355, 1974.

[14] Rosvany GIN., Prager W., "Optimal design of partially discretized grillages," *J. Mech. Phys. Solids,* vol. 24, pp. 125-136, 1976.

[15] Rozvany GIN., "Exact analytical solutions for some popular benchmark problems in topology optimization," *Structural optimization,* vol. 15, pp. 42-48, 1998.

[16] Eschenauer H., Olhoff N., "Topology optimization of continuum structures," *Applied Mechanics Reviews,* vol. 54, no. 4, pp. 331-390, 2001.

[17] Hassani B., Hinton E., "A review of homogenization and topology optimization I-homogenization theory for media with periodic structure," *Computers & Structures,* vol. 69, no. 6, pp. 707-717, 1998.

[18] Rozvany GIN., "A critical review of established methods of structural topology optimization," *Structural multidisciplinary optimization,* vol. 37, pp. 217-237, 2009.

[19] Hollister S. J., Kikuchi N., "A comparison of homogenization and standard mechanics analyses for periodic porous composites," *Computational Mechanics,* vol. 10, pp. 73-95, 1992.

[20] Fish J., Shek K., Pandheeradi M., Shephard M., "Computational plasticity for composite structures based on mathematical homogenization: Theory and practice," *Computer Methods in applied mechanics and engineering,* vol. 148, no. 1-2, pp. 53-73, 1997.

[21] Suquet P. M., Bataillon P.E., Elements of homogenization for inelastic solid mechanics. Homogenization techniques for composite media: lectures delivered at the CISM International center for mechanical sciences, Udine, Italy, 1987.

[22] Olhoff N., Lurie K. A., Cherkaev A.V., Fedorov A., "Sliding regimes of anisotropy in optimal design of vibrating plates," *International journal of solid structures,* vol. 17, no. 10, pp. 931-948, 1981.

[23] Gibianski L.V., Cherkaev A.V., "Microstructures of composites of extremal rigity and exact estimates of provided energy density (in Russian). Tech report 1155, A.F. Ioffe Physical-Technical Institute, Academy of sciences of the USSR. English translation in: Cherkaev A.V. and Kohn R.V.," Topics in mathematical modelling of composites materials, Birkhauser, New York, 1997.

[24] Bulman S., Sienz J., Hinton E., "Comparisons between algorithms for structural topology optimization using a series of benchmark studies," *Computers & structures,* vol. 79, pp. 1203-1218, 2001.

[25] Bendsoe MP, "Optimal shape design as a material distribution problem," *Structural optimization,* vol. 1, pp. 193-202, 1989.

[26] Bendsoe MP, Sigmund O, "Material interpolation schemes in topology optimization," *Archive of applied mechanics,* vol. 69, pp. 635-654, 1999.

[27] Rietz A., "Sufficiency of a finite exponent in SIMP (power law) methods," *Structural multidisciplinary optimization,* vol. 21, pp. 159-163, 2001.

[28] Rossow HP, Taylor JE, "A finite element method for the optimal design of varaible thickness sheets," *AIAA J,* vol. 11, pp. 1566-1569, 1973.

[29] Atrek E, "SHAPE: A program for shape optimization of continuum structures.," in *Software systems for structural optimization*, S. Hörnlein, Ed., Birkhauser Verlag, 1993, pp. 229-249.

[30] Xie Y, Steven G, "A simple evolutionary procedure for structural optimization," *Computers & Structures,* vol. 49, no. 5, pp. 885-896, 1993.

[31] Liu J, Parks G., Clarkson P., "Metamorphic development: a new topology optimization method for continuum structures," *Struct Multidisc Optim,* vol. 20, pp. 288-300, 2000.

[32] Eschenauer H, Kobelev V, Schumacher A., "Bubble method for topology and shape optimization of structures," *Structural optimization,* vol. 8, no. 1, pp. 42-51, 1994.

[33] Garreau S., Gillaume P., Masmoudi M., "The topological asymptotic for PDE systems: the elastic case," *SIAM Journal on control and optimization,* vol. 39, no. 6, pp. 1756-1778, 2001.

[34] Sokolowski J., Zochowski A., "On topological derivative in shape optimization," INRIA Lorraine, France, 1997.

[35] Osher S., Sethian J., "Fronts propagating with curvature dependent speed," *Journal of Computational Physics,* vol. 79, no. 1, pp. 12-49, 1988.

[36] Sethian J., Wiegmann A., "Structural boundary design via level set and immersed interface methods," *Journal of Computational Physics,* vol. 163, pp. 489-528, 2000.

[37] Osher S., Santosa F., "Level set methods for optimization porblems involving geometry and constraints: frequencies of a two-density inhomogeneous drum.," *Journal of Computational Physics,* vol. 171, pp. 272-288, 2001.

[38] Wang M., Wang X., Guo D., "A level set method for structural topology optimization," *Computer methods in applied mechanics and engineering,* vol. 192, pp. 227-246, 2003.

[39] Wang X., Wang M.Y., Guo D., "Structural shape and topology optimization in a level-set-based framework of region representation," *Struct Multidisc Optim,* vol. 27, pp. 1-19, 2004.

[40] Wang M., Wang X., ""Color" level sets: a multi-phase method for structural topology optimization with multiple materials," *Computer methods in applied mechanics and engineering,* vol. 193, pp. 469-496, 2004.

[41] Allaire G., Jouve F., Toader A., "A level-set method for shape optimization," *C. R. Acad. Sci. Paris,* vol. serie I 334, pp. 1125-1130, 2002.

[42] Allaire G., Jouve F., Toader A., "Structural optimization using sensitivity analysis," *Journal of Computational Physics,* vol. 194, pp. 363-393, 2004.

[43] Allaire G., de Gournay F., Jouve F., Toader A., "Structural optimization using topological and shape," *Control and Cybernetics,* vol. 34, no. 1, pp. 59-80, 2005.

[44] Burger M., Hackl B., Ring W., "Incorporating topological derivatives into level set methods," *Journal of computational physics,* vol. 194, pp. 344-362, 2004.

[45] Belytschko T., Xiao S., Parimi C., "Topology optimization with implicit functions and regularization," *International Journal for Numerical Methods in Engineering,* vol. 57, pp. 1177-1196, 2003.

[46] Allaire G., Jouve F., "A level-set method for vibration and multiple loads," *Computer methods in applied mechanics and engineering,* vol. 194, pp. 3269-3290, 2005.

[47] Sukumar N., Chopp D., Moes N., Belytschko T., "Modeling holes and inclusions by level sets in the extended finite element method," *Computer methods in applied mechanics and engineering.,* vol. 190, pp. 6183-6200, 2001.

[48] Wang S., Wang MY, "A moving superimposed finite element method for structural topology optimization," *International journal for numerical methods in engineering,* vol. 65, pp. 1892-1922, 2006.

[49] Amstutz S., Andra H., "A new algorithm for topology optimization using a level-set method," *Journal of computational physics,* vol. 216, pp. 573-588, 2006.

[50] Wang S., Wang M., "Radial basis functions and level set method for structural topology optimization," *International journal for numerical methods in engineering.,* vol. 65, pp. 2060-2090, 2006.

[51] Wang S.Y., Lim K.M., Khoo B.C., Wang M.Y., "An extended level set method for shape and topology optimization," *Journal of computational physics,* vol. 221, no. 1, pp. 395-421, 2007.

[52] Chen J., Shapiro V., Suresh K., Tsukanov I., "Shape optimization with topological changes and," *International Journal for numerical mehtods in engineering,* vol. 71, pp. 313-346, 2007.

[53] Wei P., Wang MY., "A piecewise constant level set method for structural topology optimization," in *7th World Congress on Structural and Multidisciplinary Optimization*, Korea, 2007.

[54] Cahn J., Hilliard J., "Free energy of a nonunifrom system. I. Interfacial free energy," *The journal of chemical physics,* vol. 28, no. 2, pp. 258-267, 1958.

[55] Allen S., Cahn J., "A microscopic theory for antiphase boundary motion and its application to antiphase domain coarsening," *Acta Metallurgica,* vol. 27, pp. 1085-1095, 1979.

[56] Bourdin B., Chambolle A., "The phase-field method in optimal design," in *IUTAM Symposium on topological design optimization of structures, machines and materials*, 2006.

[57] Bourdin B., Chambolle A., "Design-dependent loads in topology optimization," *ESAIM: Control, optimization and calculus of variations,* vol. 9, pp. 19-48, 2003.

[58] Wang MY., Zhou S., "Phase field: A variational method for structural topology optimization," *Computer Modeling in Engineering & Sciences,* vol. 6, pp. 547-566, 2004.

[59] Burger M., Stainko R., "Phase-Field Relaxation of Topology Optimization with Local Stress Constraints," *SIAM J. Control Optim,* vol. 45, no. 4, pp. 1447-1466, 2006.

[60] Takesawa A., Nishiwaki S., Kitamura M., "Shape and topology optimization based on the phase field method ans sensitivity analysis.," *Journal of computational physics,* vol. 229, no. 7, pp. 2697-2718, 2010.

[61] Rong JH., Liang QQ, "A level set method for topology optimization of continuum," *Computer methods in applied mechanics and engineering,* vol. 197, pp. 1447-1465, 2008.

[62] Mei Y., Wang X., "A level set method for structural topology optimization and its applications," *Advances in engineering software,* vol. 35, no. 7, pp. 415-441, 2004.

[63] Liu Z., Korvink J.G., Huang R., "Structure topology optimization: fully coupled level set method via FEMLAB," *Struct. Multidisc. Optimization,* vol. 29, pp. 407-417, 2005.

[64] Luo Z., Tong L., Wang M.Y., Wang S., "Shape and topology optimization of compliant mechanisms using a parameterization level set method.," *Journal of computational physics,* vol. 227, no. 1, pp. 680-705, 2007.

[65] Park S., Min S., Yamasaki S., Nishiwaki S., Yoo J., "Magnetic actuator design using level set vased topology optimization," *IEEE Transactions on magnetics,* vol. 44, no. 11, pp. 4037-4040, 2008.

[66] Luo Z., Tong L., Luo J., Wei P., Wang M.Y., "Design of piezoelectric actuators using a multiphase level set method of piecewise constants.," *Journal of computational physics,* vol. 228, pp. 2643-2659, 2009.

[67] Luo Z., Tong L., Ma H., "Shape and topology optimization for electromechanical microactuators using level set methods," *Journal of computational physics,* vol. 228, pp. 3173-3181, 2009.

[68] Sigmund O., Petersson J., "Numerical instabilities in topology optimization: A survey on procedures dealing with checkerboards, mesh-dependencies and local minima," *Structural optimization,* vol. 16, pp. 68-75, 1998.

[69] Sigmund O., "Materials with prescribed constitutive parameters: An inverse homogenization problem.," *International journal of solid structures,* vol. 31, pp. 2313-2329, 1994.

[70] Petersson J., Sigmund O., "Slope constrained topology optimization," *International journal of numerical methods in Engineering,* vol. 41, pp. 1417-1434, 1998.

[71] Boyd S., Vandenberghe L., Convex optimization, United Kingdom: Cambridge university press, 2004.

[72] Sigmund O., "A 99 line topology optimization code written in Matlab," *Structural Multidisciplinary Optimization,* vol. 21, pp. 120-127, 2001.

[73] V. G., Numerical optimization techniques for engineering design., Santa Barbara: McGraw-Hill, 1984.

[74] M. Bendsoe, "Optimal shape design as a material distribution problem," *Structural optimization,* vol. 1, pp. 193-202, 1989.

[75] Rosvany GIN., "Exact analytical solutions for some popular benchmark problems in topology optimization," *Structural optimization,* vol. 15, pp. 42-48, 1998.

[76] Delfour M., Zolesio J., "Oriented distance function and it evolution equation for initial sets with thin boundary," *SIAM Journal of Control Optimization,* vol. 42, no. 6, pp. 2286-2304, 2004.

[77] Goldberg D.E., Genetic algorithms in search, optimization and machine learning, Addison Wesley, 1989.

[78] Hajela P., Lee E., "Genetic algorithm in truss topological optimization," *International journal of solids and structures,* vol. 32, no. 22, pp. 3341-3357, 1995.

[79] Czech C., "Thesis: Design of Meta-Materials outside the homogenization limit using multiscale analysis and topology optimization.," Clemson University, Clemson, 2012.

[80] Pindera M.J., Khatam H., Drago A., Bansal Y., "Micromechanics of spatially uniform heterogeneous media: A critical review and emerging approaches.," *Composites: Part B,* vol. 10, pp. 349-378, 2009.